TWEAK AND cIAP1 MEDIATE ALTERNATIVE NF-κB SIGNALLING TO PROMOTE MYOGENESIS

Nadine Jessica Adam

A thesis submitted to the
Faculty of Graduate and Postdoctoral Studies
in partial fulfillment of the requirements for the
MSc degree in Biochemistry

Department of Biochemistry, Microbiology, and Immunology
Faculty of Medicine
University of Ottawa

ABSTRACT

The NF-κB family of transcription factors can be activated through canonical (classical) or non-canonical (alternative) signalling pathways, which are regulated by the redundant ubiquitin ligases, cellular inhibitor of apoptosis 1 and 2 (cIAP1 and cIAP2). While the canonical NF-κB pathway is needed for myoblast proliferation, it is inactivated during myoblast differentiation. However, the non-canonical NF-κB pathway is a major factor in promoting myoblast fusion, which is crucial to the processes of myogenesis and muscle repair. Ablation of cIAP1 levels through a chemical antagonist such as a SMAC-mimetic compound (SMC) activates non-canonical signalling to enhance myogenesis. The cytokine TNF-like weak inducer of apoptosis (TWEAK) has also been shown to activate primarily the alternative NF-κB pathway when signalling through its receptor Fn14. Here I show that alternative NF-κB signalling activity, stimulated by the addition of TWEAK or loss of cIAP1, can promote myogenesis. I also demonstrate that TWEAK is an endogenous myokine produced by myoblasts to promote their own differentiation, and suggest that targeting the alternative NF-κB pathway, with SMAC-mimetics or recombinant TWEAK for example, would be of therapeutic value in the repair and regeneration of muscle for various myopathies.

ACKNOWLEDGMENTS

First, thanks to Dr. Korneluk for giving me this wonderful opportunity, for his excellent supervision, and for putting up with the fact that my blots are always currently running when he asks to see them. Thanks also to Dr. LaCasse for allowing me to throw around ideas, and especially thanks for being willing to proofread and for providing constructive criticism and lots of reading materials. Thanks to all the Korneluk lab members, both past and present, especially Martine St. Jean, Janelle Chabot, Dr. Hapsa Mamady, and Dr. Emeka Enwere. Thanks also to my committee members Drs. Dennis Bulman and Alex MacKenzie for their advice and support.

Thanks to my parents for all their encouragement, and for bravely crossing the world with their three daughters. I wouldn't be who or where I am today without you guys. I hope to be able to repay you one day for everything you've done for me! Ek is baie lief vir julle! Jeanelle: thanks for looking out for me over the years and for sparking my interests in so many of my passions. Sharon: thanks for always providing hugs and laughter, for your love and support and your positive attitude. Thanks to Donnie and Jan for being like a second set of parents, for constant encouragement and for tons of laughs as well; and to the rest of the Kavanaghs for all the fun, the great food, and the constant laughs.

Most of all, thanks to Kevin for being my best friend, my biggest fan, and my strongest ally. None of this would've been possible without your constant support, encouragement, and love. And I'm not just referring to letting me borrow the Pilot. You push me to do my best in everything I pursue, and I couldn't imagine having completed this project without you. Ek is lief vir jou, Kevintjie. Last but definitely not least, thanks to Laila, our peepster sleeps, for unconditional love, warm cuddles, and for keeping me company during the writing period. It would've been RUFF without you!

TABLE OF CONTENTS

LIST OF ABBREVIATIONS

bFGF	Basic fibroblast growth factor
bHLH	Basic helix-loop-helix
BIR	Baculoviral IAP repeat
BSA	Bovine serum albumin
cIAP1/2	Cellular inhibitor of apoptosis ½
CTX	Cardiotoxin
DMD	Duchenne muscular dystrophy
DMEM	Dulbecco's modified eagle medium
FBS	Fetal bovine serum
Fn14	Fibroblast growth factor-inducible 14
HGF	Hepatocyte growth factor
IAP	Inhibitor of apoptosis
IκB	Inhibitor of kappa B
IKKα	Inhibitor of kappa B Kinase-α
IKKβ	Inhibitor of kappa B Kinase-β
MHC	Myosin heavy chain
mTWEAK	Murine TWEAK
NF-κB	Nuclear factor-κB
NIK	NF-κB interacting protein
PBS	Phosphate-buffered saline
PCR	Polymerase chain reaction
PFA	Paraformaldehyde
RING	Really interesting new gene
SMAC	Second mitochondrial activator of caspases
SMC	Smac-mimetic compound
RIP1	Receptor interacting protein 1
RT-qPCR	Reverse transcriptase quantitative PCR
TBS-T	Tris-phosphate buffered saline with Tween
THD	TNF homology domain
TNFα	Tumour necrosis factor-α
TNFR	Tumour necrosis factor receptor
TRAF	TNFR-associated factor
TWEAK	Tumour necrosis factor-like weak inducer of apoptosis
WT	Wildtype
YY1	Yin Yang 1

LIST OF FIGURES

LIST OF TABLES

Chapter 1 – Introduction

1.0 Overview

Recent studies in muscle biology have shown a role for NF-κB signalling in the differentiation of muscle stem cells into terminally differentiated myofibres, the unit cell of muscle. The E3 ubiquitin ligase cIAP1, a member of the inhibitor of apoptosis (IAP) family of proteins, has been shown to be a mediator of this signalling cascade. A recent study from our lab specifically linked the cytokine TWEAK to the promotion of alternative NF-κB signalling through cIAP1 sequestration, thereby causing an increase in myoblast fusion (Enwere et al., 2012). For this project, I wanted to further study the downstream signalling that TWEAK activates, and its larger role in the general process of myoblast fusion.

1.1 Skeletal muscle and associated pathologies

Skeletal muscle comprises an important system with vital roles in voluntary locomotion and posture, and this tissue develops from mesenchymal stem cells and their descendants, known as satellite cells (Mauro, 1961). These mononuclear cells will differentiate and fuse into a multinucleated syncytium termed a myofibre. Embryonic development involves formation of nascent myotubes from satellite cells, but at a certain point development of new myofibres ceases, with focus placed on expanding existing fibres instead. In adult skeletal muscle little growth occurs, with satellite cells mainly functioning to maintain homeostasis of muscle in response to injury and general wear due to use. In adult muscle, the number of fibres within a muscle remains consistent, with any changes in muscle mass being due to alterations in the size of individual pre-existent fibres, where increases are referred to as hypertrophy. A tightly regulated balance between muscle breakdown and repair must be

maintained, and thus numerous debilitating illnesses surrounding the skeletal muscle system exist, including genetic issues leading to structural malformations, and muscle loss due to the general process of aging, disuse or chronic illness such as cancer.

Atrophy of skeletal muscles is highly prevalent and encompasses multiple conditions, including starvation, disuse due to immobilization, or the presence of an adverse disease state. Though similar in that a loss of overall muscle mass is present, each of these conditions has characteristic biochemical and histological features associated with it. Disuse atrophy, or atrophy due to limb immobilization, is characterized by decreases in muscle fibre size, with no accompanying changes in the number of muscle fibres present. At the molecular level, muscles undergoing atrophy also show decreases in overall protein content; this involves both decreased synthesis and increased degradation of protein within the muscle (Loughna et al., 1986; Thomason and Booth, 1989). While muscle disuse atrophy is typically caused by muscle unloading, cachexia is a much more severe syndrome, with atrophy caused by the release of cachectic factors as a secondary effect of chronic illness such as cancer (Fearon et al., 2006), chronic heart failure (Anker and Coats, 1998), and many others. In cachectic muscle, different fibre types are targeted for degradation depending on the underlying illness (Acharyya et al., 2005; Mendell and Engel, 1971). The general loss of muscle mass is also considered a fairly common feature of the aging process, in which case it is termed sarcopenia (Evans, 1995; Evans and Wayne, 1993). This process also involves marked decreases in both fibre number and size, leading to loss of overall muscle strength as well as an estimated loss of 5% muscle mass every ten years once an individual reaches the age of 40 (Carmeli et al., 2002; Forbes and Reina, 1970; Tzankoff and Norris, 1977). While exercise can restore muscle atrophy from disuse, recovery from atrophy due to cachexia and sarcopenia is often much more difficult, and these conditions often ultimately lead to frailty.

In addition, nutritional supplementation does not reverse muscle loss due to cachexia (Evans et al., 1985).

In some cases, predisposing genetic mutations can cause pathologies involving skeletal muscle. The group of muscle disorders known as muscular dystrophies involve progressive skeletal muscle degeneration accompanied by general weakness. Perhaps the most studied and indeed most common neuromuscular disorder is Duchenne muscular dystrophy (DMD), an X-linked disorder estimated to affect 1 in 3500 males causing severe and progressive muscle wasting beginning at a very young age. Most individuals affected by this disorder die by their mid-20s due to cardiac or respiratory failure. In comparison with healthy, unaffected muscle tissue where the multinucleated myofibres are consistent in size and have peripherally located nuclei, dystrophic muscle fibres display large variation in size and are centrally nucleated, a sign of regeneration. This phenotypic difference is due to the constant cycle of degeneration and regeneration of the muscle fibres. Satellite cells are responsible for the regeneration process. In muscular dystrophy where regeneration is continuous, the regenerative capacity was initially thought to be lost due to depletion of the satellite cell pool within the muscle (Collins et al., 2005). However, more recent work has shown that satellite cell numbers are increased in patients with DMD (Bankolé et al., 2013; Kottlors and Kirschner, 2010), and points to a dysfunctional muscle environment hindering the regenerative capabilities of satellite cells instead (Boldrin et al., 2015).

Due to the prevalence of muscle wasting both pathologically and as a result of the aging process, muscle physiology is an important topic of study. Satellite cells, their proliferation and maintenance of myofibres through the general process of myogenesis may indeed present a possible therapeutic intervention into these diseases.

1.2 Satellite cells and myogenesis

Satellite cells are located surrounding muscle fibres beneath the basal lamina and are crucial for the continuous maintenance and repair thereof (Grounds, 1998; Moss and Leblond, 1971; Schultz, 1996). Satellite cells can be identified easily in skeletal muscle through their expression of a myriad of myogenic transcription factors including Pax7, Pax3, Myf5, and many others. Pax7 is commonly used as the main marker of satellite cells since it is expressed in both quiescent and proliferative cells (Seale et al., 2000), and is found in a multitude of species including mouse and human (McLoon and Wirtschafter, 2003). Pax3 by contrast is only found within certain muscles in the body. Pax3 and Pax7 are paired-homeobox transcription factors that are key players in a multitude of organ development processes. In satellite cells, quiescence is associated with expression of Pax7 but no expression of any of four known myogenic regulatory factors (MRFs), namely MyoD (Davis et al., 1987), Myf5 (Braun et al., 1989), myogenin (Edmondson and Olson, 1989), and MRF4 (Braun et al., 1990; Miner and Wold, 1990; Rhodes and Konieczny, 1989). These helix-loop-helix factors are able to convert non-myogenic cells such as fibroblasts into myoblast-like cells capable of myogenesis. Activation from quiescence involves rapid upregulation of MyoD or Myf5, and these factors are coexpressed for the entire period that the satellite cells are proliferative (Cornelison and Wold, 1997). Following satellite cell activation, the cells become myoblasts and are capable of rapid proliferation after which they will undergo differentiation to form nascent myotubes once more. The cells entering differentiation downregulate Pax7, Pax3 and Myf5 (Zammit et al., 2006), and begin to express myogenin and Mrf4. The characteristic multinucleated myotubes found within skeletal muscle form from the alignment of myogenin-containing myoblasts, and their subsequent fusion. Those returning to quiescence downregulate MyoD, and maintain levels of Pax7. A model

representing the general differentiation and fusion process is shown in **figure 1**. Much work has been done in looking at each of these factors within the overall process of skeletal muscle formation. Pax7 has been shown through studies of Pax7 deficient mice to be crucial for the maintenance of the satellite cell colony, since these mice have sufficient numbers of satellite cells at birth but over time are severely depleted therein and rarely survive to adulthood (Kuang, 2006; Oustanina et al., 2004; Relaix, 2006). While MyoD and Myf5 are required for commitment to differentiation and the process of proliferation of myoblasts respectively, knockout mice have shown that its partner can compensate for loss of either factor alone during the initial development process, but neither protein can sustain both roles throughout adulthood (Rudnicki et al., 1993). Myogenin, in contrast, is not needed until later in the differentiation process for the formation of the myotubes themselves. Indeed, it has been shown that loss of myogenin at later stages leads to a loss of muscle mass (Knapp et al., 2006).

Satellite cells form the regenerative potential of skeletal muscle in humans. Studies have shown that activation of these cells is triggered by muscle injury, either by normal use or through outside injury (Grounds, 1998). Thus, a constant supply of satellite cells is necessary for maintenance of muscle mass. Indeed, it has been shown that skeletal muscle loses much of its regenerative capacity throughout aging, and this has been linked to a loss in the activity of satellite cells. The molecular trigger for activation of satellite cells from quiescence is still a topic of study. Sphingosine-1-phosphate is one implicated molecule due to its role in re- entry into the cell cycle as well as the general loss of regeneration capabilities when its synthesis is blocked (Nagata et al., 2006). Studies have also shown that some triggers cause intracellular changes within the fibre, resulting in release of hepatocyte

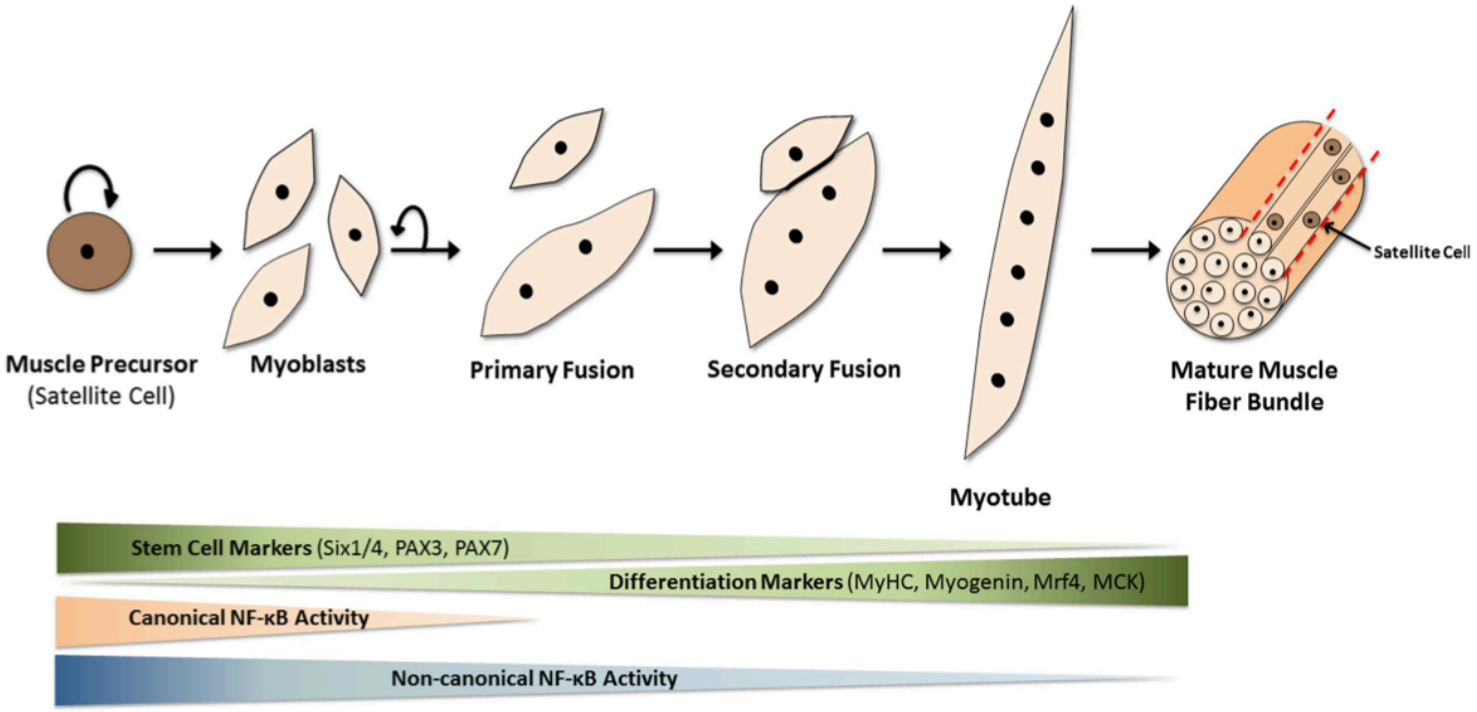

Fig. 1. Representative model of the process of myoblast differentiation, including activation from satellite cells through to the final mature muscle fibres.
During this process, stem cell markers including Pax3 and Pax7 are downregulated, while differentiation markers such as myosin heavy chain (MHC), myogenin and Mrf4 are upregulated (Enwere et al., 2014).

growth factor (HGF), which has been suggested to activate satellite cells through its receptor c-Met (Wozniak and Anderson, 2007). Additionally, growth factors released by fibroblasts, such as fibroblast growth factors (FGFs) have been studied due to their activation of MAPK signalling, which has been shown to regulate the cell cycle of satellite cells (Jones et al., 2005).

In recent years, the role of the nuclear factor κB (NF- κB) signalling pathway in the process of myogenesis has been intensely studied in relation to both the role of the pathway in normal, healthy muscle development and maintenance as well as dysregulation of the pathway in muscle pathology. For example, one therapy that has produced some benefit in DMD children is the use of high dose glucocorticoids, which have anti-NF-κB activity and are immunosuppressive. They prevent somewhat the fibrotic damage in muscles that occurs upon repeated rounds of degeneration and regeneration seen in these fragile, dystrophin-deficient muscle cells.

1.3 NF-κB signalling

The NF-κB pathway has implications in a wide range of cellular processes including muscle wasting (Cai et al., 2004) and other pathologies such as muscular dystrophy (Acharyya et al., 2007), and has a wide range of target genes such as the inflammatory cytokine TNF-α, also referred to as cachectin (Collart et al., 1990; Shakhov et al., 1990) and Stat5a (Hinz et al., 2002). The NF-κB family of proteins comprises a set of five transcription factors, namely RelA (p65), RelB, c-Rel, p105/p50 and p100/p52. In general, NF-κB signalling can be split into two pathways, termed the classical/canonical and alternative/non-canonical and illustrated in **figure 2**. Classical signalling involves the heterodimer of RelA

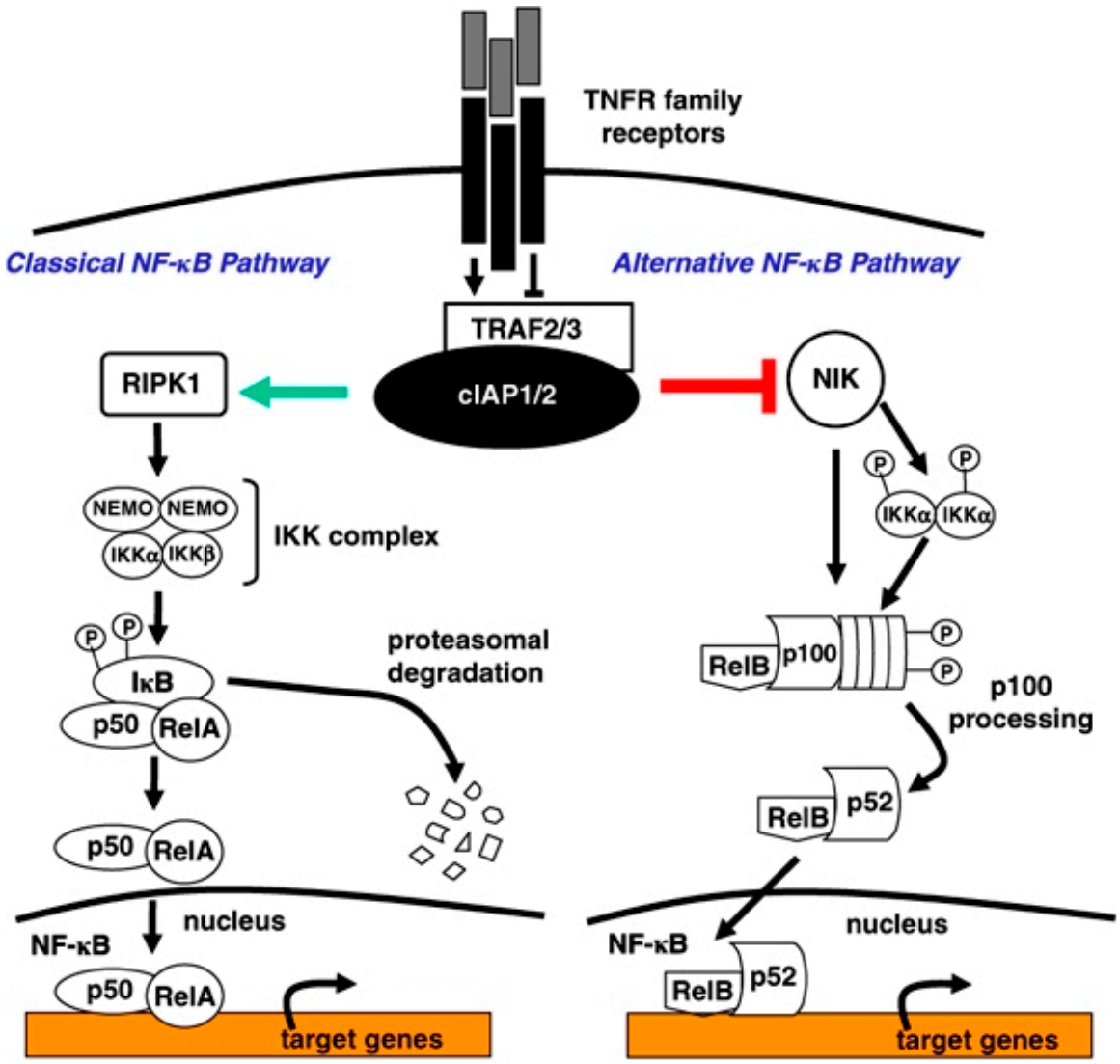

Fig. 2. Signalling cascades of the classical (left) and alternative (right) NF-κB pathways. The cellular inhibitors of apoptosis (cIAPs) have an important role in regulation thereof. Under basal conditions, the cIAPs ubiquitinate NIK for degradation, inhibiting the alternative pathway. In contrast, ubiquitination of RIP1 activates the classical pathway (LaCasse et al., 2008).

and p50, which prior to a stimulatory signal is sequestered in the cytoplasm due to association with the inhibitor of κB protein (IκB). Activation of the classical NF-κB pathway has been linked to stimuli such as TNFα. Upon initiation of the pathway by this activating stimulus, an inhibitor of κB kinase (IKK) complex consisting of NEMO, IKKα and IKKβ phosphorylates IκB, leading to its polyubiquitination and subsequent proteasomal degradation. The p50:RelA dimer is then free for nuclear translocation, and there can activate target genes. In contrast, the alternative NF-κB pathway involves the heterodimer of RelB and p100, which is sequestered in the cytoplasm until p100 is processed into p52. This processing is performed following activation of NF-κB inducing kinase (NIK), which in turn activates IKKα. Similar to canonical signalling, IKKα then phosphorylates p100, triggering its proteolytic processing into the smaller p52. The RelB:p52 heterodimer is then able to translocate to the nucleus to activate target genes of the alternative pathway. Of note, cellular inhibitor of apoptosis 1/2 (cIAP1/2), E3 ubiquitin ligase proteins in the IAP family, act as central regulators of the classical and alternative NF-κB signalling pathways. These proteins ubiquitinate both receptor-interacting protein 1 (RIP1) and NIK. Ubiquitination of RIP1 allows the formation of a scaffold complex that recruits other factors, and leads to downstream recruitment of NEMO to the IKK complex. cIAP1/2 thus activate classical NF-κB signalling. In contrast, ubiquitination of NIK leads to its proteasomal degradation, thus inactivating any downstream alternative NF-κB signalling.

NF-κB signalling is known to be active at low levels in many cell lines. However, myoblasts have been shown to present constitutive activation of NF-κB in culture. The interplay between the classical and alternative pathways plays a large role in the switch from myoblast proliferation to differentiation. As shown in **figure 3**, the classical pathway is

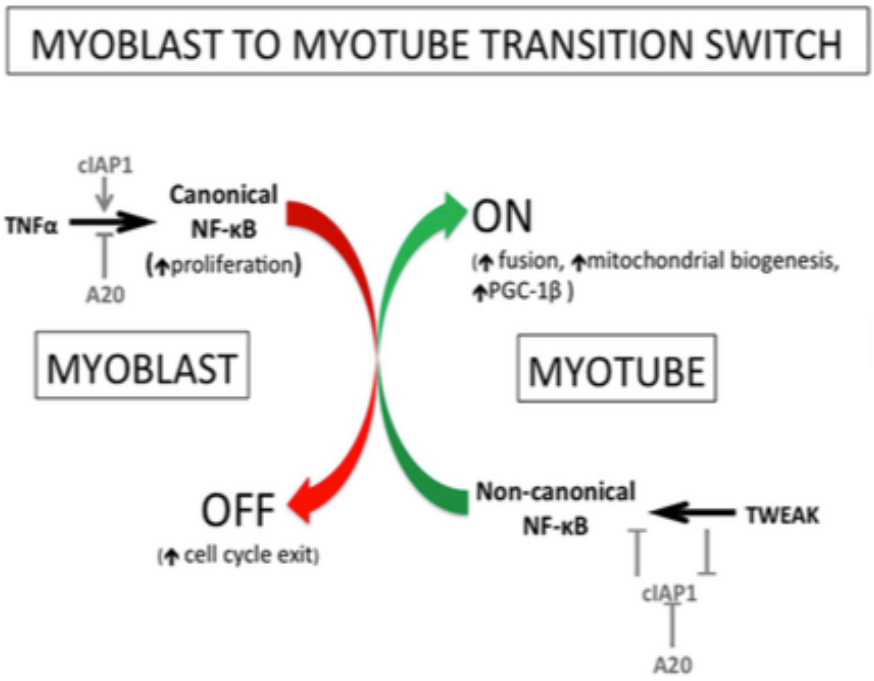

Fig. 3. The switch from canonical (classical) to non-canonical (alternative) NF-κB signalling is vital for a switch from proliferation to differentiation in myoblasts. Classical signalling is highly linked with proliferation and cell cycle progression, and must be turned off for differentiation to occur. Alternative signalling is linked with fusion and mitochondrial biogenesis (Enwere et al., 2014).

mainly active during proliferation, and is switched off once the cells enter differentiation. The alternative pathway is mainly activated during the differentiation process. There are many ways in which the classical pathway maintains the cells in a proliferative state. In myoblasts, the p50/p65 heterodimer of the classical pathway has been shown to be involved in cell progression into the S phase of the cell cycle via transcriptional regulation of cyclin D1 (Guttridge et al., 1999). It has also more recently been shown that p65 acts as an enhancer to the kinase CDK4, which complexes with cyclin D1 to initiate the G1/S transition; p65 also stabilizes the cyclin D1 protein itself (Dahlman et al., 2009). In addition to stimulating cell proliferation, the classical pathway has also been implicated in destabilization of MyoD mRNA, preventing protein expression, which is crucial for the differentiation of skeletal muscle (Guttridge et al., 2000). More recently it has also been shown that the p50/p65 heterodimer upregulates expression of Yin Yang 1 (YY1), which associates with members of the Polycomb repressive complex to inhibit expression of certain muscle-specific genes including MHCIIb (Wang et al., 2007). In contrast to the classical pathway, the alternative signalling pathway has recently been implicated in activating myogenesis and increased fusion through increased processing of p100 to p52 due to loss of activity of a protein known as cIAP1 (Enwere et al., 2012) and in myotube maintenance (Bakkar et al., 2008).

1.4 The IAP family of proteins and cIAP1

The inhibitors of apoptosis proteins (IAPs) are a family of related proteins that play a large role in cell survival and apoptosis. The IAP genes were initially discovered within a baculovirus conferring the virus the ability to prevent host cell apoptosis following infection (Crook et al., 1993). This family of proteins is characterised by the presence of at least one

baculoviral IAP repeat (BIR) domain, which in some cases confers the protein the ability to bind and competitively inhibit caspases, thereby inhibiting the process of apoptosis. These BIR domains are 70 amino acid long zing-binding regions (Birnbaum et al., 1994; Hinds et al., 1999; Sun et al., 1999). Some IAPs also contain a ubiquitin ligase zinc finger domain known as the Really Interesting New Gene (RING) domain. The combination of caspase binding as well as caspase ubiquitination triggering their proteasomal degradation allows for potent inhibition of apoptosis, though the IAPs have many other important roles as well. Two highly studied IAPs are cellular inhibitors of apoptosis (cIAP) 1 and 2. Each of these contains three BIR domains near their N terminus as well as a RING domain near their C terminus. The cIAPs are TNF-receptor associated factor- (TRAF) binding proteins, which facilitates their role in many protein complexes involving receptors and substrates. They are critical transducers of immune signalling by acting as E3 ubiquitin ligases for proteins such as RIP1, RIP2, and many others.

1.5 cIAP1 and SMAC-mimetic compounds in myogenesis

Since the IAPs are ubiquitous and potently inhibit cell death, a process that is often necessary for proper development, natural inhibitors are present within cells and can be triggered by a pro-apoptotic stimulus. One such inhibitor is the protein second mitochondrial activator of caspases (Smac), a mitochondrial protein released following a pro-apoptotic stimulus. Once released into the cytoplasm, its truncated form binds the BIR3 domain of cIAP1/2, directly inhibiting their caspase-binding abilities specifically with respect to caspase-9 and also leading to their autoubiquitination and thus proteasomal depletion, activating the process of apoptosis. Due to this crucial and powerful role of Smac, compounds mimicking its IAP binding, known as Smac-mimetic compounds (SMCs) have

been developed and are being clinically evaluated for the treatment of cancer. SMCs mediate the rapid degradation of the cIAPs, and in doing so cause the activation of alternative NF-κB pathways and transient activation of the classical NF-κB pathway (Enwere et al., 2012).

cIAP1/2 have been shown to play an important role in the NF-κB signalling pathway and subsequently in the overall process of myogenesis (Enwere et al., 2012; Varfolomeev et al., 2012). Binding of an NF-κB activating molecule to its membrane-bound receptor causes the formation of a receptor-signalling complex consisting of the receptor, TNF receptor-associated factor 2 (TRAF2), and cIAP1/2. Following formation of the complex, the IAPs ubiquitinate receptor interacting kinase I (RIP1) through lysine-63 linkages of the ubiquitin peptide, leading to the downstream recruitment of NEMO to the IKK complex. In some cells, cIAPs bound to TRAF2/TRAF3 complexes ubiquitinate NIK through lysine-48 linkages, which potently activates proteasomal degradation of NIK. Following an NF-κB-activating signal, the sequestration of the cIAPs to the TNF/TNF receptor (TNFR) complex causes stabilization of NIK, and thus resulting in the activation of the alternative NF-κB signalling pathway.

In looking at the involvement of the NF-κB pathway in myogenesis with respect to the role of cIAP1/2, interesting results have emerged. It was recently shown that myoblasts from cIAP1$^{-/-}$ mice form large, highly branched and hypernucleated myotubes despite also being delayed in exiting the cell cycle following stimulation to differentiate (Enwere et al., 2012). These myoblasts also exhibited higher basal levels of alternative and classical NF-κB signalling. Additionally, wildtype myoblasts were treated with a SMC, which was shown to activate both the classical and alternative NF-κB pathways shortly following the onset of

differentiation (Enwere et al., 2012). Through knockdown of various components of the alternative pathway in cIAP1$^{-/-}$ myoblasts, it was shown that the alternative pathway was crucial to the phenotype seen in the differentiated myotubes. Altogether these results suggested antagonism between the two pathways during differentiation, where the classical pathway prevents myogenesis and must be shut down, while the alternative pathway drives the process, at least initially (Enwere et al., 2012).

1.6 TWEAK/Fn14 and NF-κB signalling

Another protein recently linked to the NF-κB signalling pathway within the process of myogenesis is TNF-like weak inducer of apoptosis (TWEAK, TNFSF12). TWEAK and its receptor fibroblast growth factor-inducible 14 (Fn14, TNFRSF12A) are a fairly novel pair of proteins in the tumour necrosis factor (TNF) and TNF-receptor (TNFR) family of proteins respectively. Despite being considered a member of the TNFR family, however, Fn14 does not bear much homology to its other family members with respect to its sequence, and is the smallest member with only 102 amino acids in the final processed transmembrane form. It does contain an extracellular cysteine-rich repeat region known to be characteristic of TNFR proteins, and was thus verified as a member of this family of proteins in 2001 (Feng et al., 2000; Wiley et al., 2001). Additionally, it contains a cytoplasmic TNF receptor-associated factor (TRAF)-binding domain capable of binding TRAF-1, -2, -3, and -5, which have been shown to be involved in downstream signalling (Brown et al., 2003; Wiley et al., 2001). Like many other TNF family members, TWEAK is synthesized as a type II transmembrane protein but is also found as a smaller, secreted form arising from proteolytic processing. The full-length TWEAK protein consists of 249 amino acids divided into three domains, namely a cytoplasmic domain near the N-terminus, a transmembrane domain, and the TNF

homology domain (THD) near the C-terminus. A small, 50-amino acid stalk region separates the THD from the transmembrane region, and comprises two furin endoprotease consensus sequences, suggesting furin-mediated processing into the secreted form of the protein (Chicheportiche et al., 1997).

Interestingly, a study of the TNF and TNFR families initially showed the TWEAK/Fn14 pair to bind only one another, forming no binding pairs with any of the other family members (Bossen et al., 2006). However, numerous other studies have indicated binding relationships with factors outside of these families. One outside binding event of note is that of TWEAK and CD163, a scavenger receptor cysteine-rich (SRCR) protein that is exclusive to monocytes or macrophages (Bover et al., 2007; Kristiansen et al., 2001). TWEAK has also been shown to cause effects in cells that do not express Fn14, such as by regulating the differentiation of RAW264.7 macrophages (Polek et al., 2003). Additionally, Fn14 has been implicated in canonical NF-κB signalling independent of TWEAK binding (Brown et al., 2003, 2013).

The TWEAK/Fn14 binding pair and subsequent signalling has been the subject of many studies over recent years, and has been implicated in liver disease, cancer, and muscle pathology. Of note, TWEAK signalling has been linked with activation of both the classical and alternative NF-κB pathways, though this activation is dose-dependent. High levels of soluble TWEAK have been shown to be linked with the classical NF-κB pathway via downstream phosphorylation of the IκB protein leading to its proteolytic degradation (Brown et al., 2003). However, these high levels have been identified as more representative of pathological levels as opposed to physiological levels. At levels more representative of physiological concentrations, TWEAK has been shown to strongly activate the alternative pathway (Enwere et al., 2012; Roos et al., 2010). This activation is similar to many other

activators of the alternative pathway, where upon ligand/receptor binding, TRAF2, TRAF3, and cIAP1/2 are recruited to the intracellular portion of the membrane-bound receptor forming a protein complex. Formation of this complex activates cIAP1/2 ubiquitination of TRAF3 on the K48 residue, ultimately inactivating the entire complex (Liao et al., 2004). This in turn means that cIAP1/2 no longer target NIK for degradation, leading to downstream activation of p100 and its subsequent processing into p52, and therein activation of the alternative NF-κB pathway and its targets. This sequence of events is modeled in **figure 4.** In addition to sequestration and thus inactivation of cIAP1/2, TWEAK signalling has also been shown to activate proteasomal and lysosomal degradation of TRAF2, TRAF3, and cIAP1/2 (Enwere et al., 2012; Vince et al., 2008). Activation of the alternative pathway by TWEAK involves stabilization of NIK, which must be translated *de novo* and accumulate; thus, this signalling is only evident several hours after onset. In contrast, activation of classical NF-κB signalling via IκB degradation is rapid, occurring within minutes.

Recently it was shown that membrane-bound TWEAK can activate downstream NF-κB signalling in a juxtacrine signalling process (Brown et al., 2010). One comprehensive study on various forms of TWEAK showed differences in downstream signalling depending on the nature of the TWEAK protein itself. Soluble TWEAK, whether produced recombinantly or through proteolytic processing, and whether trimeric or fused to be hexameric in quaternary structure, strongly induced alternative NF-κB processing. The membrane-bound unprocessed form of TWEAK was also shown to do so. However, while trimeric soluble TWEAK variants were unable to stimulate classical NF-κB signalling even at significantly high doses, oligomeric variants of TWEAK showed strong activation thereof at low doses (Roos et al., 2010).

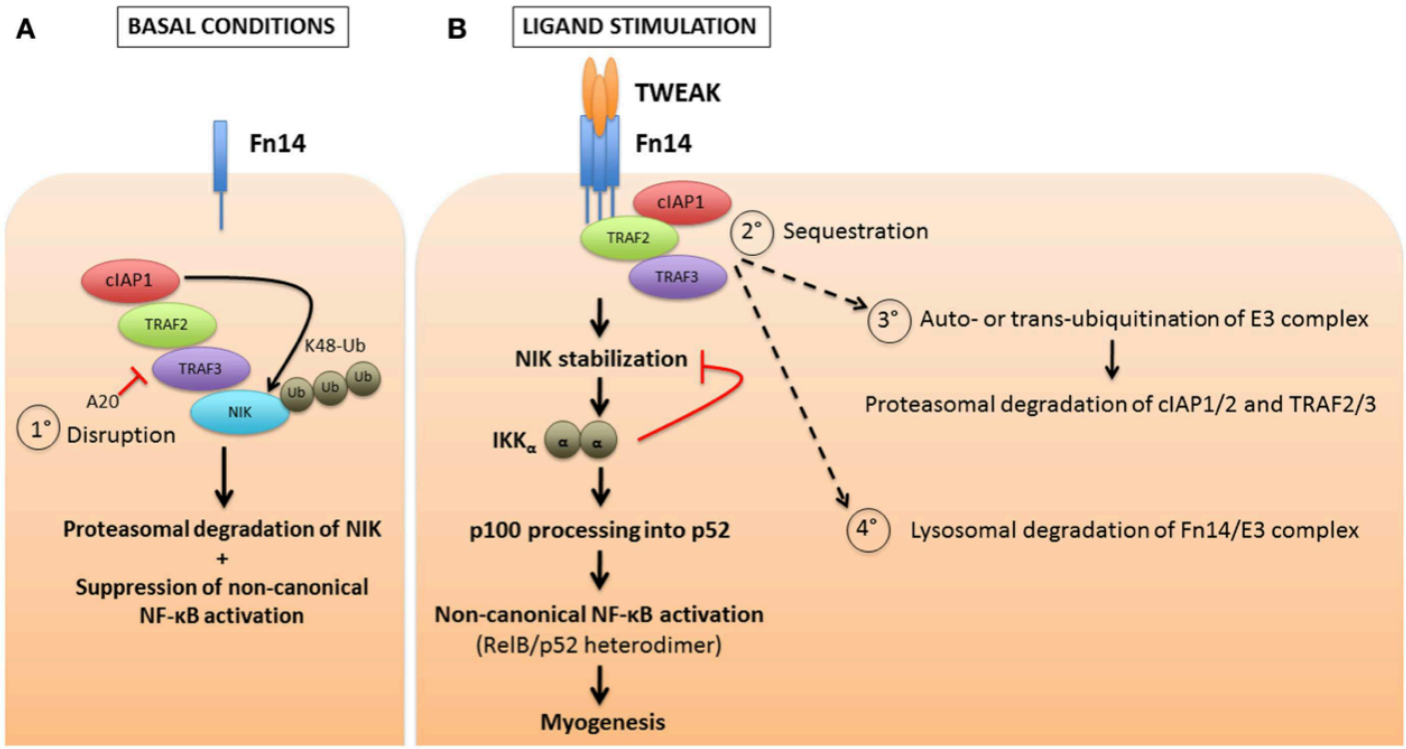

Fig. 4. Model of TWEAK-mediated activation of alternative NF-κB signalling through cIAP1 sequestration. Under basal conditions, cIAP1 ubiquitinates NIK, leading to its proteasomal degradation and thereby suppresses alternative NF-κB signalling. Upon binding of TWEAK to Fn14, cIAP1, TRAF2, and TRAF3 form a membrane-bound complex with Fn14, leading to loss of cIAP1 functioning and thus stabilization of NIK, which activates downstream signalling and increased fusion (Enwere et al., 2014).

1.7 TWEAK/Fn14/cIAP1 and muscle regeneration

As mentioned in section 1.5, recent *in vitro* studies have shown that cIAP1$^{-/-}$ primary myoblasts constitutively exhibit higher levels of NF-κB signalling in culture. Upon differentiation, robust fusion occurs, where these cells form large, hypernucleated myotubes due to the enhanced alternative NF-κB signalling. It was also shown that treating wildtype myoblasts with low doses of exogenous TWEAK triggered similar robust alternative NF-κB activation, while higher doses activated both arms of the NF-κB pathway (Enwere et al., 2012). *In vivo*, cIAP1$^{-/-}$ mice regenerated muscle fibres slightly larger in size when compared to control mice following injury involving intramuscular injection of the snake venom cardiotoxin (CTX), which induces focal muscle injury. This effect was not as robust as the size disparity seen in formed myotubes *in vitro.* Mice treated with TWEAK through a surgically inserted micro-osmotic pump showed much more significant increase in regenerated fibre size (Enwere et al., 2012).

Despite these reportedly positive effects of TWEAK on regeneration, contradictory results are extensive within the literature. Firstly, muscle regeneration has been shown to be more rapid within TWEAK$^{-/-}$ mice when compared to wildtype controls, while slower comparative regeneration is seen in genetically engineered mice expressing TWEAK at constitutively high levels under control of a muscle-specific promoter (Mittal et al., 2010a). Further contradictory results lie in the fact that Fn14$^{-/-}$ mice are significantly impaired in their regenerative capacity (Dogra et al., 2007; Enwere et al., 2012). Fn14 upregulation has also been linked to muscle atrophy and regeneration (Dogra et al., 2007; Mittal et al., 2010b). The negative effects of TWEAK on muscle regeneration discussed by numerous studies (Dogra et al., 2006; Ogura et al., 2013) are in line with negative effects on the regeneration of many other organ types. However, as discussed in a recent review by Enwere *et al.*, these studies

focus on systems where TWEAK is present at pathologically high levels, or is being overexpressed constitutively in all cell types via transgenes (Enwere et al., 2014); this combined with many experiments highlighting the positive effects of TWEAK on progenitor proliferation again suggests the dose-dependent nature of TWEAK signalling (Girgenrath et al., 2006; Jakubowski et al., 2005; Novoyatleva et al., 2010).

1.8 Project rational and hypothesis

As discussed in section 1.5, cIAP1/2 and the NF-κB signalling pathway in general pose potential therapeutic targets for the treatment of muscle disease. Indeed, muscle atrophy has already been linked to upregulation in NF-κB. Numerous other factors are likely involved in cIAP1/2 and NF-κB signalling and the general process of myogenesis. Using cIAP1$^{-/-}$ myoblasts (in comparison to wild-type myoblasts) I investigated a subset of 59 possible fusion- or NF-κB-related factors initially through a low-throughput siRNA screen to determine their role in the hyperfusion phenotype that is seen following differentiation. Hits from this screen were further studied to elucidate the role of cIAP1/2 and NF-κB in myoblast differentiation and fusion. It is hypothesized that the TWEAK/Fn14 signalling axis is involved in this pathway and plays a significant role in myogenesis via activation of the NF-κB signalling pathway. This signalling axis may pose a potential therapeutic target for the treatment of muscle pathologies.

1.9 Statement of objectives

1. Elucidate factors involved in hyperfusion phenotype observed in cIAP1$^{-/-}$ myoblasts through a 59-candidate low-throughput siRNA screen targeting factors previously shown to be involved in differentiation/fusion or NF-κB signalling
2. Further study effects of TWEAK knockdown on process of myoblast differentiation and fusion, to show its role in the fusion process
3. Analyze effects of exogenous TWEAK and the SMC LCL161 on myoblast differentiation and fusion, phenotypically and molecularly to further show their involvement in fusion and in activation of NF-κB signalling

Chapter 2 - Materials and methods

2.1 Myoblast cell culture

2.11 Mouse models

Female C57BL/6 mice were used as wildtype mice for all experiments, and were obtained from Charles River Laboratories Inc. cIAP1$^{-/-}$ mice were acquired from Dr. Mak (Toronto, ON, Canada) as previously characterised (Conze et al., 2005). Mice were housed in the University of Ottawa Animal Care and Veterinary Services Facility in accordance with the Institutional Animal Care and Use Committee guidelines.

2.12 Isolation of mouse primary myoblasts

Young female mice (<8 weeks old) were used for all primary myoblast isolations. Mice were euthanized by cervical dislocation, and muscles from the hind limbs were isolated, cut longitudinally and placed in phosphate-buffered saline (PBS). Muscles were then transferred to a 6cm dish containing 8 mL of syringe-filtered 0.2% type I collagenase (Invitrogen) and dispase (Roche) in DMEM (ATCC) containing penicillin/streptomycin. The plate was sealed using autoclave tape and placed in a shaker at 37 °C and 75 RPM for 2 – 2.5 hours, at which point muscles were triturated with a 10 mL pipette until fully dissociated. This solution was then passed through a 74 µm Netwell filter (VWR) for complete removal of undigested tissues. Volume was increased to 20 mL with DMEM and the solution was centrifuged at 3000 xg for 5 minutes. The supernatant was discarded and the cells resuspended in 20 mL of DMEM. This solution was again centrifuged for 5 minutes at 3000 xg. The cell pellet was resuspended in 10 mL of 10% donor equine serum

(HyClone) and 5 ng/mL bFGF (Cedarlane) in DMEM. This was transferred to a tissue culture-coated 10 cm plate and left in the incubator (5% CO_2, 37°C) for 1 hour, referred to as "pre-plating". At this point the suspension was transferred to one well of a 6-well plate pre-coated with Matrigel (Sigma) diluted at 1:10 in cold DMEM. The cells were left for 2 days to allow for proper attachment, and then passaged in full growth media (10% donor equine serum, 20% fetal bovine serum, 10 ng/mL bFGF, 2 ng/mL HGF in DMEM) for proliferation. Media was changed daily during growth. Cells were again "pre-plated" prior to seeding experimental plates to remove fibroblast contamination.

2.13 Differentiation assays and treatments

In order to study differentiation, myoblasts were plated and left to attach for 24 hours. At this point, media was changed to differentiation media (10% donor equine serum in DMEM) for the extent of differentiation. Plates were put in an IncuCyte ZOOM® (Essen) for 72 hours for time-lapse phase-contrast microscopy monitoring at 10x magnification at 37°C and 5% CO_2. Treatments during differentiation were started once differentiation media was added to cells. For TWEAK treatment, purified murine TWEAK (mTWEAK) was obtained from R&D Systems Inc. (Minneapolis) and resuspended in 0.1% bovine serum albumin (BSA) in PBS. 20 μL of the appropriate concentration was pipetted into the media in order to have a final concentration within the media of either 10 ng/mL or 100 ng/mL. The Smac-mimetic LCL161, a monomeric SMC from Novartis currently in trials as a cancer therapeutic (Infante et al., 2014), was diluted in DMEM at the appropriate concentration and spiked into media at a volume of 20 μL in order to have a final concentration within the media of 1000 μM.

2.14 Transfection using siRNA

siRNAs were obtained from Dharmacon (see **Table 2** in Appendix for sequences and catalogue numbers) and resuspended at 20 μM. Plated cells were transfected with appropriate siRNA at a final concentration of 25 nM using Lipofectamine RNAiMAX (BioRad) for a period of 24 hours. Transfections were set up in 400 μL/well of OPTIMEM, left at room temperature for 5 minutes, and mixed with 1.6 mL of growth media containing serum and growth factor concentrations appropriate for the total 2 mL volume. Following the 24-hour transfection period, cells were rinsed with PBS, switched to differentiation media, and monitored in the IncuCyte Zoom® for 72 hours.

2.15 Immunocytochemistry of myotubes

Plastic cover slips (Thermanox®) were placed in the wells of a 12-well plate and coated with 1:10 diluted Matrigel. Cells were then plated onto these at 75000 cells per well, and left for 24 hours to attach. At this point, cells were switched to differentiation media and the appropriate treatment was added, as discussed in section 2.13. Cells were monitored until optimal differentiation occurred, at which point coverslips were fixed with 3.7% paraformaldehyde (PFA) for 15 minutes. Cells were then permeabilized with a solution of 0.2% triton X-100 for 15 minutes at room temperature. After three 1-minute rinses with PBS, cover slips were incubated with blocking buffer solution (0.5% BSA, 0.3% Triton X-100) for 15 minutes at room temperature. 1:250 diluted primary mouse anti-MHC antibody prepared in blocking buffer was then added overnight at 4°C. Cover slips were rinsed with blocking buffer three times for 5 minutes each, followed by incubation in 1:100 diluted Alexafluor 594 anti-mouse secondary antibody in blocking buffer for 1 hour at room temperature. After more rinses with blocking buffer, cover slips were mounted on a glass

slide using mounting medium (Agilent Technologies) and dried overnight. Immunofluorescence was visualized using a x-Cite® series 120Q excitation light source (Excelitas Technologies) and cellSense Entry software (Olympus).

2.2 Protein collection and analysis

2.21 Cell protein extraction

At the appropriate times, plates were rinsed once with cold PBS, and cells were scraped in 1 mL of cold PBS. Cells were pelleted by spinning at 21.1 xg at 4°C, and supernatant was aspirated off. Cell pellets were then frozen at -80°C until processing. For protein extraction, pellets were resuspended with a protease inhibitor cocktail (Roche) prepared in whole-cell lysis buffer. Suspensions were passed through 27-gauge needle to completely dissociate any fibres. Protein content of lysates was quantified through a BioRad DC^{TM} protein assay, a common Lowry assay for protein concentration, at which point lysates were stored at -20°C until further use.

2.22 Western immunoblotting

Measured quantities of protein from cell lysates were used to prepare 20 μg samples, which were diluted with 2x Laemmli Sample Buffer (Bio-Rad) prepared with β-mercaptoethanol. Very diluted samples were diluted with 5x Laemmli buffer in order to keep the final volume under 40 μL. Prepared samples were then run in 7% polyacrylamide gels at a voltage of 120V for 1.5 hours, or until the dye front reached the bottom.

Protein was transferred to 0.45 μm nitrocellulose membranes through using a TE 77 semi-dry transfer apparatus (GE Healthcare Life Sciences) for 90 minutes at 600 mA.

Membranes were then blocked with Odyssey® Blocking Buffer (Li-Cor) diluted 1:1 in PBS for 30 minutes, followed by overnight incubation in the appropriate primary antibody at 4°C. After removal of primary antibody, membranes were washed with Tris-phosphate buffered saline with Tween (TBS-T) four times for 7 minutes, then PBS for 7 minutes, after which they were incubated with the appropriate secondary antibody for 1 hour at room temperature. After one more 7-minute wash with each TBS-T and PBS, blots were scanned on the infrared scanner Odyssey (Li-Cor) using Image Studio software (Li-Cor). Fluorescence images were captured using either AlexaFluor 680 or 800 secondary antibodies. β-tubulin levels were used as a standard for loading.

2.23 Antibodies

Antibodies to p100/52, p65, and P-p65 were polyclonal rabbit antibodies obtained from Cell Signalling Technology. The antibody to MHC was obtained from Developmental Studies Hybridoma Bank (Iowa City, Iowa). The RIAP1 antibody was a rabbit anti-rat cIAP2 polyclonal antibody, which detects both cIAP1 and 2 in mouse, rat, and human samples (Holcik et al., 2002).

2.3 mRNA extraction and analysis

2.31 RNA extraction

For RNA extraction, cell pellets were collected as discussed in section 2.21 and frozen at -80°C until extraction. Total cell RNA was extracted using an Absolutely RNA Miniprep Kit (Agilent Technologies) as per the manufacturer's directions, and eluted in a

final volume of 20 μL RNase-free water. Isolated RNA was quantified using the Eppendorf Biophotometer at an OD of 260nm. RNA was then kept at -80°C until further use.

2.32 Reverse Transcriptase Quantitative Polymerase Chain Reaction (RT-qPCR)

1 μg extracted RNA was run through a reverse transcriptase reaction using iScript™ Advanced cDNA Synthesis Kit for RT-qPCR reagents following the manufacturer's instructions (Bio-Rad). These samples were then diluted 1:100 for further use in qPCR on a Mastercycler RealPlex^2 instrument with accompanying RealPlex Software (Eppendorf). qPCR plates were set up such that each sample was run in triplicate using SsoAdvanced Universal SYBR® Green Supermix reagents (Bio-Rad) following the manufacturer's instructions. Primers were used at 10 μM, and blanks were made for each primer. B2M was used as the standardizing control gene. Relative gene expression was calculated via $\Delta\Delta C_q$ values, where a sample's quantification cycle (C_q) numbers are first normalized to the standardizing control gene, and subsequently normalized to the control, untreated sample (see Haimes et al., 2010). Primer sequences are shown in **Table 3**, in the appendix.

2.4 Statistical analyses and graphing

All quantitative data are represented as mean of triplicate runs. $\Delta\Delta C_q$ values were calculated via Excel (Microsoft). Graphs were generated via GraphPad Prism 5 (GraphPad Prism Software, La Jolla, CA).

Chapter 3 – Results

3.1 In vitro 59-candidate low-throughput screen for factors involved in myoblast differentiation and fusion

Following a comprehensive review of literature pertaining to NF-κB targets and mediators as well as factors generally associated with myogenesis and myoblast fusion in some capacity, a list of 59 candidate genes were identified and chosen for a small-scale low-throughput screen. For the purposes of this screen, cIAP1$^{-/-}$ myoblasts were used due to their robust differentiation phenotype, allowing for clear and easy detection of differences in phenotypic result. This siRNA-based screen experiment was performed as per **figure 5**, and results were analyzed and scored based on myotube branching, a phenotypic result of the fusion process. Scores had possible values of -2 for severe inhibition of differentiation/fusion resulting in zero branch points, -1 for hindered differentiation/fusion resulting in 1-10 branch points, 0 for no difference from non-targeting control ranging from 11-19 branch points, or +1 for increased differentiation/fusion resulting in ≥20 branch points. The list of candidates and their scoring results are summarized in **table 1**. Representative pictures of the non-targeting control as well as each score are shown in **figure 6.** Of note, knockdown of NIK and p100 resulted in scores of -1. Additionally, knockdown of TWEAK and Fn14 resulted in scores of -1 and -2 respectively. TWEAK was chosen as a target for further investigation due to these findings.

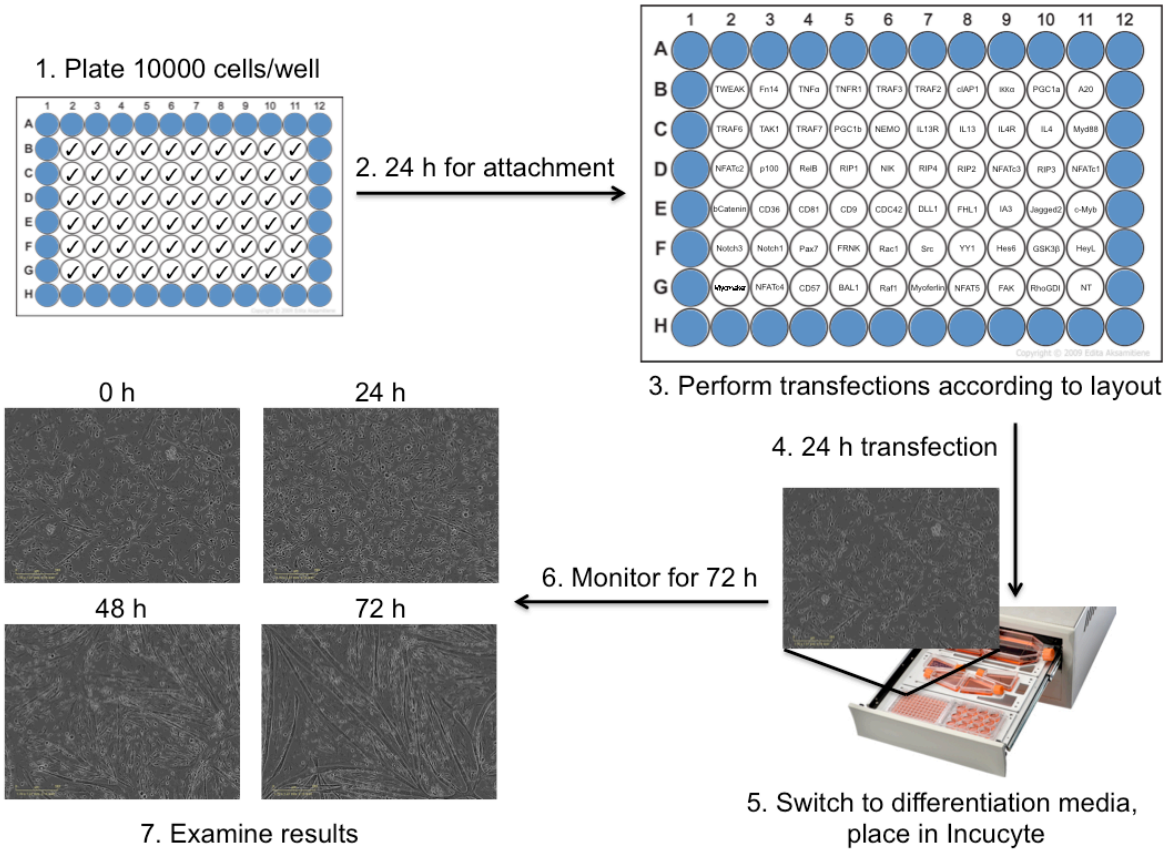

Fig. 5. Representation of procedure for 59-candidate low-throughput screen.
cIAP1$^{-/-}$ cells were plated on a 96-well format, transfected for 24 hours using Dharmacon siRNAs. Next, they were switched to differentiation media and monitored for 72 hours of differentiation via the IncuCyte ZOOM® by capturing phase contrast images at hourly intervals. Resulting images were exported and used for eventual scoring. Outer wells (shown in blue) were filled with sterile water to humidify the plate. Screen was run on three separate 96-well plates so as to have 3 replicates.

Table 1. Summarized results of 59-candidate low-throughput siRNA screen of primary myoblast differentiation.

Target	Gene symbol	Number of branch points in picture frame	Screen score*
Non-targeting	**N/A**	18	0
TNFSF-TNFRSF and alternative NF-κB			
TWEAK	TNFSF12	1	-1
Fn14	TNFRSF12A	0	-2
TNF-α	TNFA	0	-2
TNFR1	TNFRSF1A	25	+1
TRAF2	TRAF2	3	-1
TRAF3	TRAF3	26	+1
TRAF6	TRAF6	15	0
TRAF7	TRAF7	11	0
TAK1	MAP3K7	17	0
A20	TNFAIP13	16	0
PGC1a	PPARGC1A	8	-1
PGC1b	PPARGC1B	12	0
cIAP1	BIRC2	2	-1
IKKα	CHUK	26	+1
RelB	RELB	28	+1
p100	NFKB2	2	-1
NIK	MAP3K14	2	-1
RIP1	RIPK1	15	0
RIP2	RIPK2	8	-1
RIP3	RIPK3	9	-1
IKKg/NEMO	IKBKG	18	0
Other Cytokines			
IL4	IL4	17	0
IL4R	IL4R	0	-2
IL13	IL13	19	0
IL13R	IL13RA1	5	-1
MyD88	IL13RA2	24	0
Calcineurin / NFAT			
NFATc1	NFATC1	17	0
NFATc2	NFATC2	17	0
NFATc3	NFATC3	16	0
NFATc4	NFACTC4	3	-1
NFAT5	NFAT5	10	0
Myoferlin	MYOF	16	0
Beta-catenin factors			
GSK3b	GSK3B	1	-1
bCatenin	CTNNB1	17	0

Notch and target genes			
Notch1	NOTCH1	5	-1
Target	**Gene symbol**	**Number of branch points in frame**	**Screen score***
Notch3	NOTCH3	0	-2
Jagged2	JAG2	17	0
DLL1	DLL1	36	+1
Hes6	HES6	0	-2
HeyL	HEYL	18	0
Pax7	PAX7	25	0
Adhesion factors			
CD9	CD9	2	-1
CD81	CD81	18	0
CD57	B3GAT1	22	+1
CD36	CD36	21	+1
Ia3	ITGA3	**	**
Miscellaneous			
Myomaker	TMEM8C	2	-1
BAL1	BAL1	19	0
YY1	YY1	**	**
c-Myb	MYB	3	-1
FHL1	FHL1	10	0
Cdc42	CDC42	15	0
RhoGDI	ARHGDIA	5	-1
cRaf/Raf1	RAF1	17	0
Rac1	RAC1	0	-2
FAK	PTK2	10	0
Src	SRC	10	0
FRNK	PTK2B	13	0

* Scores were assigned as follows: -2 for complete absence of branch points, -1 for 1-9 branch points, 0 for 10-19 branch points, +1 for ≥20 branch points.

** Indicates targets unable to be scored due to technical issues.

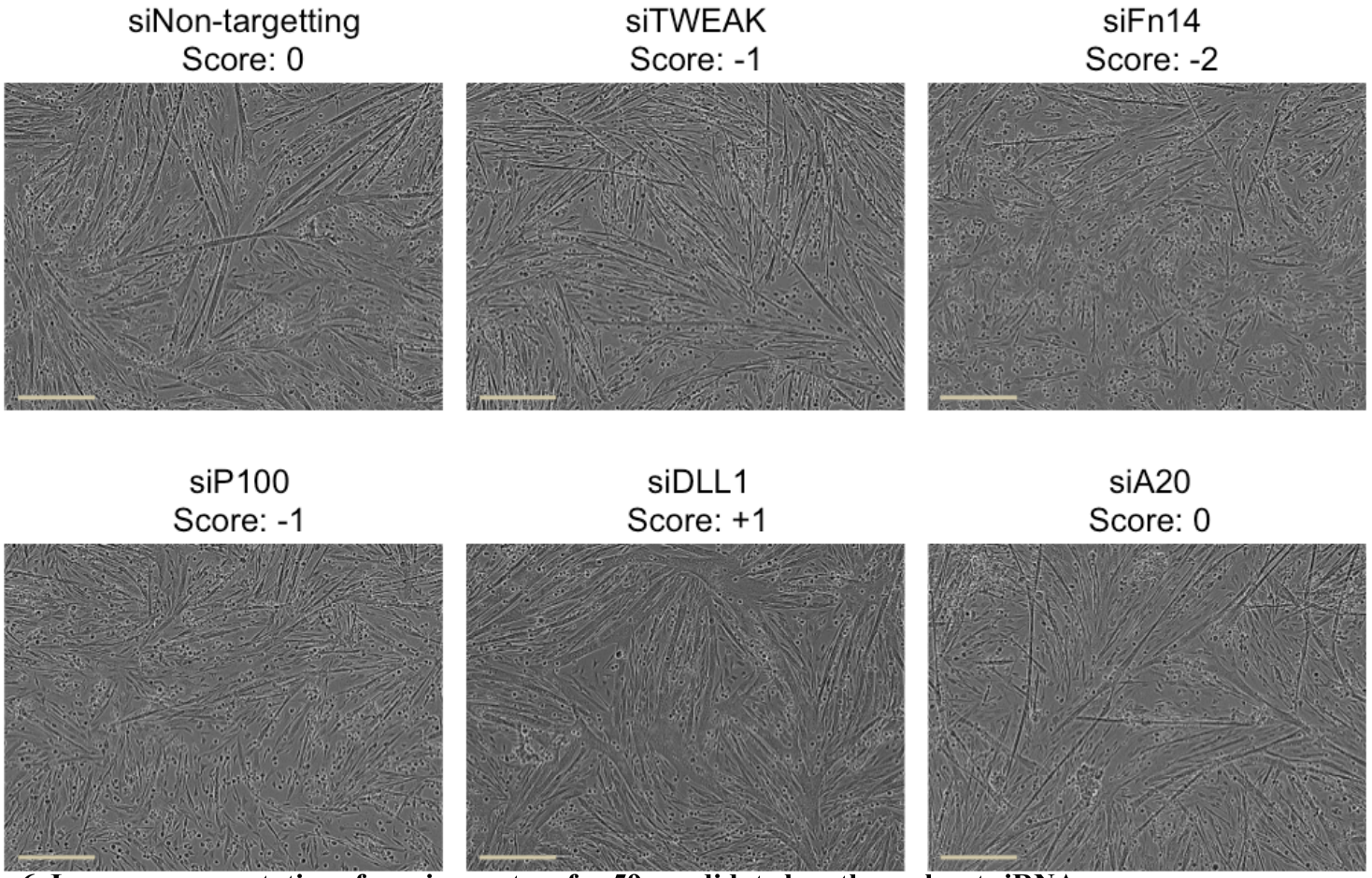

Fig. 6. Images representative of scoring system for 59-candidate low-throughput siRNA screen.
cIAP1$^{-/-}$ cells were plated on a 96-well format, transfected for 24 hours using Dharmacon siRNAs. Next, they were switched to differentiation media and monitored for 72 hours of differentiation via the IncuCyte ZOOM® by capturing phase contrast images at hourly intervals.. Scores were based on the number of branch points present within the frame, and were assigned as follows: -2 for complete absence of branch points, -1 for 1-9 branch points, 0 for 10-19 branch points, +1 for ≥20 branch points. Scale bar represents 300 μm. Experiment was repeated at least three times; images represent one replicate.

3.2 TWEAK is endogenous to myoblasts, and is involved in fusion

Following the outcome of TWEAK knockdown in the siRNA screen, RNA from wildtype primary myoblasts was isolated every 24 h during differentiation for a total of 72 h. RT-qPCR was performed using B2M as a standardizing control. It was thus confirmed that TWEAK mRNA is present within primary myoblasts over the course of their differentiation, as shown in **figure 7.** Interestingly, it is also evident that levels of TWEAK mRNA decrease over the course of differentiation.

To further investigate the results of TWEAK knockdown in differentiating myoblasts, knockdown of TWEAK using the Dharmacon siRNA pool was repeated with wildtype myoblasts to confirm the results. This was also performed on a larger scale using a 6-well plate monitored by the IncuCyte ZOOM® microscope in a tissue culture incubator over a 72 hour period. The pooled siRNA was also deconvoluted to investigate each individual siRNA sequence independently. Resulting phenotypes are shown in **figure 8.** All four individual siRNAs as well as the pool resulted in the presence of less myotubes following 48 hours of differentiation. Western blot analysis using myosin heavy chain (MHC) as a marker of differentiation was performed on samples from the 0, 24, 48, and 72 hour timepoints following transference to differentiation media, and is shown in **figure 9A**. No significant difference in the levels of differentiation was evident. However, all four deconvoluted siRNAs as well as the pool resulted in a delay in differentiation, as evident from the lower levels of MHC present within 24 hours of transference to differentiation media. To verify that these effects were in fact due to knockdown of TWEAK mRNA, RT-qPCR was performed to analyze mRNA levels following the 24-hour transfection period, prior to the addition of differentiation media. These results are shown in **figure 9B,** and illustrate that the siRNA pool does cause a decrease in TWEAK mRNA levels, as do siRNA #3 and #4.

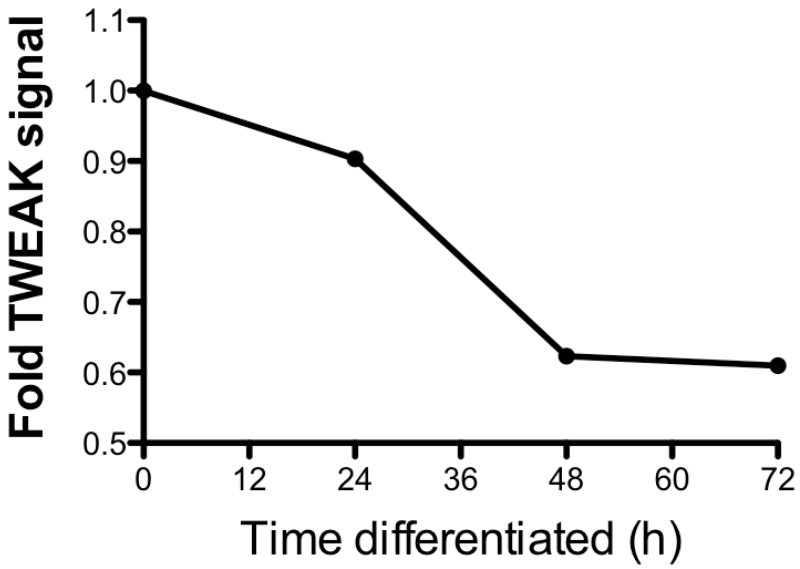

Fig. 7. TWEAK is endogenously produced in mouse primary myoblasts.
RNA was extracted from wildtype myoblasts every 24 hours over a 72-hour differentiation period. mRNA was quantified via RT-qPCR using Universal SYBR® Green Supermix reagents (Bio-Rad). B2M mRNA levels were used as a standardizing control. Experiment was repeated at least three times; values represent one replicate.

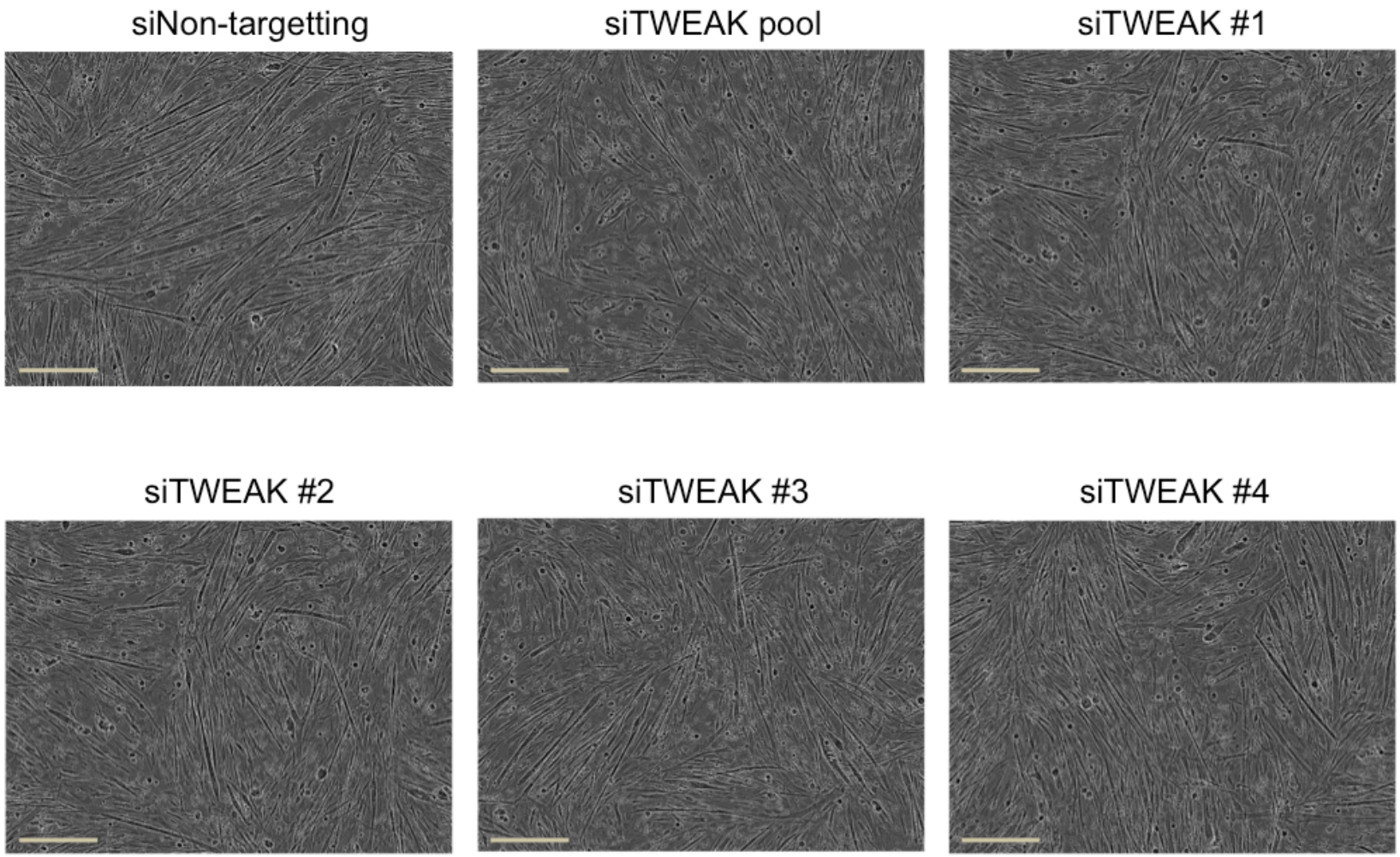

Fig. 8. siRNA-mediated TWEAK knockdown in primary mouse myoblasts leads to a loss of fusion.
Phase contrast images of wildtype myoblasts differentiated for 48 hours following a 24-hour transfection with the specified siRNA. Images were obtained at 10X magnification via IncuCyte ZOOM® apparatus. Scale bar represents 300 μm. Experiment was repeated at least three times; images represent one replicate.

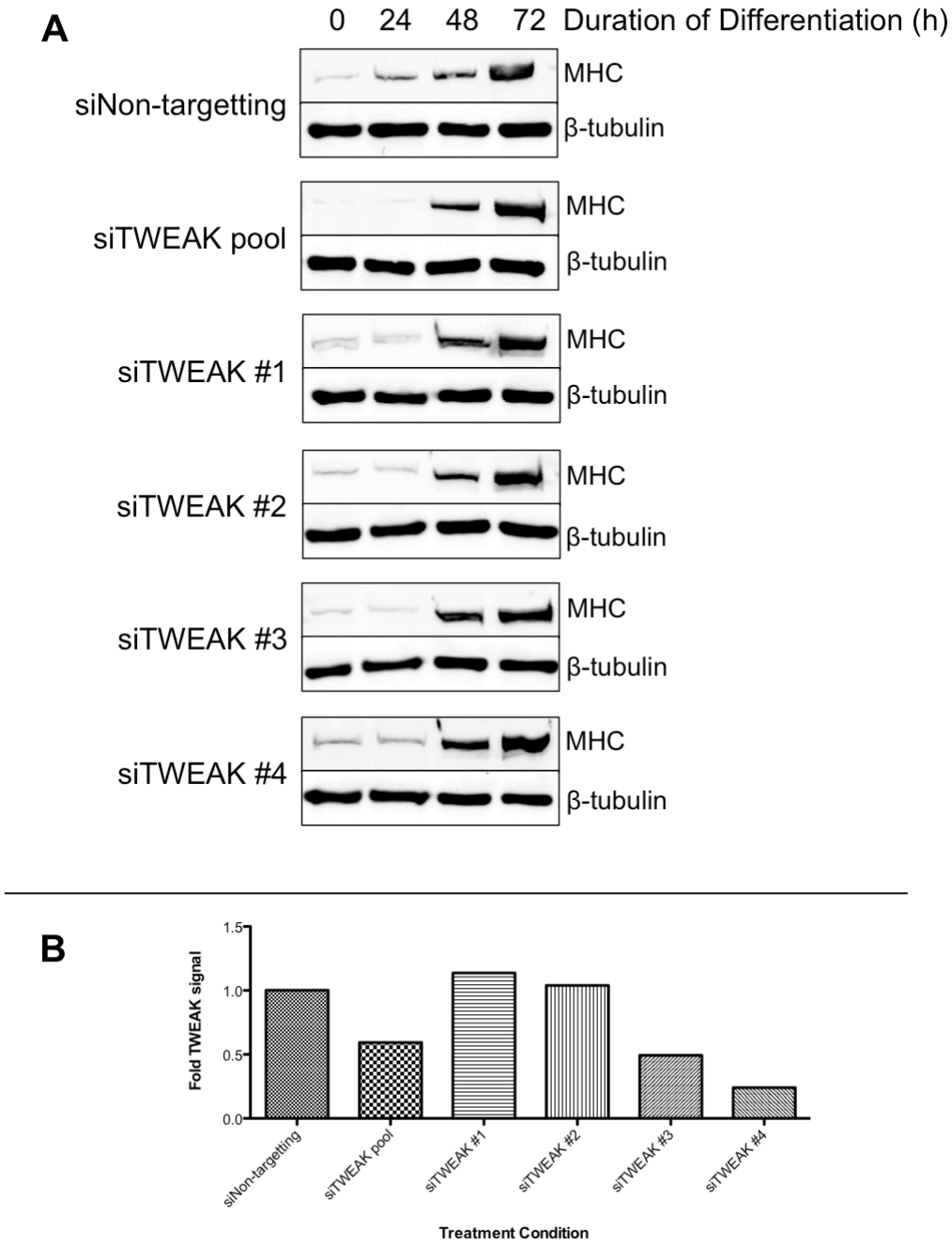

Fig. 9. siRNA-mediated knockdown of TWEAK does not impact differentiation, and is effectively knocking down TWEAK mRNA.

A: Western blotting analysis where myosin heavy chain (MHC) represents a marker of differentiation over the 72-hour differentiation period, with levels increasing as cells differentiate into myotubes. No significant differences are evident between treatment conditions. B: RT-qPCR analysis of TWEAK mRNA levels in order to verify knockdown, which was on-target. mRNA was quantified via RT-qPCR using Universal SYBR® Green Supermix reagents (Bio-Rad). B2M mRNA levels were used as a standardizing control. Experiment was repeated at least three times; images and values represent one replicate.

3.3 Exogenous mTWEAK promotes myoblast fusion

Previous work in our lab has shown a dose-dependent response of myoblast differentiation to exogenous murine TWEAK (mTWEAK), with a dosage of 10 ng/mL resulting in a hyperfusion phenotype similar to that of cIAP1$^{-/-}$ myoblasts but a dosage of 100 ng/mL resulting in an inhibition in the differentiation process (Enwere et al., 2012). Furthermore, as mentioned in section 3.2, loss of TWEAK through siRNA-mediated knockdown seemingly led to inhibition of fusion suggesting a role for TWEAK in the process of myogenesis Thus, in order to further analyze this proposed role, wildtype myoblasts were treated with either a low dose (10 ng/mL) of mTWEAK, a high dose (100 ng/mL) of mTWEAK, or PBS as a control (referred to as "untreated"), and monitored via the IncuCyte ZOOM® apparatus and images analyzed with its accompanying software. Hourly images were captured and analyzed over the course of 72 hours of differentiation, and the entire set of images was assessed to determine which timepoint represented optimal differentiation. These images were also compiled into a video format for ease of viewing (see attached CD). From this close analysis, it was shown that 100 ng/mL of exogenous TWEAK, though seemingly causing negative effects on differentiation, in fact promotes a hyperfusion phenotype to such an extent that formed myotubes contract, sheering off of the Matrigel-coated plates, thus no longer being successfully captured by the imaging software.

Previous work has also shown that loss of cIAP1 in wildtype myoblasts through a Smac-mimetic compound also resulted in a hyperfusion phenotype (Enwere et al., 2012). Following from the preliminary results of the exogenous mTWEAK, the experiment was repeated, including an additional treatment with the Smac-mimetic compound LCL161, a clinical SMC candidate from Novartis, in order to study the molecular mechanisms at work. Differentiation was also separately monitored over a 72-hour period via IncuCyte ZOOM®.

As shown in **figure 10**, both untreated myoblasts and those receiving 10 ng/mL mTWEAK reached optimal differentiation at the 72-hour timepoint, though the final product of the low dose condition contained more branch points and thicker tubes. In comparison, the high dose condition produced similar results as seen in previous work at the 72-hour timepoint. However, the phenotype was observed at 40 hours into differentiation, the optimal tubes for this condition, mimic those seen in the LCL161-treated myotubes. These tubes are thick, and contain many branch points. In order to more easily visualize formed myotubes, immunocytochemistry was performed in a separate experiment by targeting MHC on cells plated to cover slips and fixed after 48 hours of differentiation. Resulting images are shown in **figure 11,** and show a large, multinucleated and branched myotube forming following treatment with 100 ng/mL mTWEAK. Somewhat smaller yet branched and multinucleated tubes are seen following treatment with 10 ng/mL mTWEAK and 1000 nM LCL161. Small, unbranched tubes are seen for untreated wildtype myoblasts.

In addition to a qualitative phenotypic analysis, protein lysates were collected from differentiating myoblasts over the course of the 72-hour differentiation period. Western blot analysis of these samples was performed, where MHC was once again used as a marker for differentiation. As shown in **figure 12A**, no significant differences are evident in levels of MHC when comparing the low dosage of mTWEAK so its untreated control, though it can be noted that MHC levels increase at an earlier timepoint with the TWEAK treatment. Under high dose conditions, however, MHC levels are much lower by the end of the 72-hour differentiation period. No significant differences are evident for LCL161-treated myoblasts, though a slight delay in the increase of MHC levels is evident. In order to confirm proper functioning of the SMC compound LCL161, degradation of cIAP1/2 was assessed via the RIAP1 antibody. As is clearly shown in **figure 12B,** treatment with LCL161 at 1000 nM

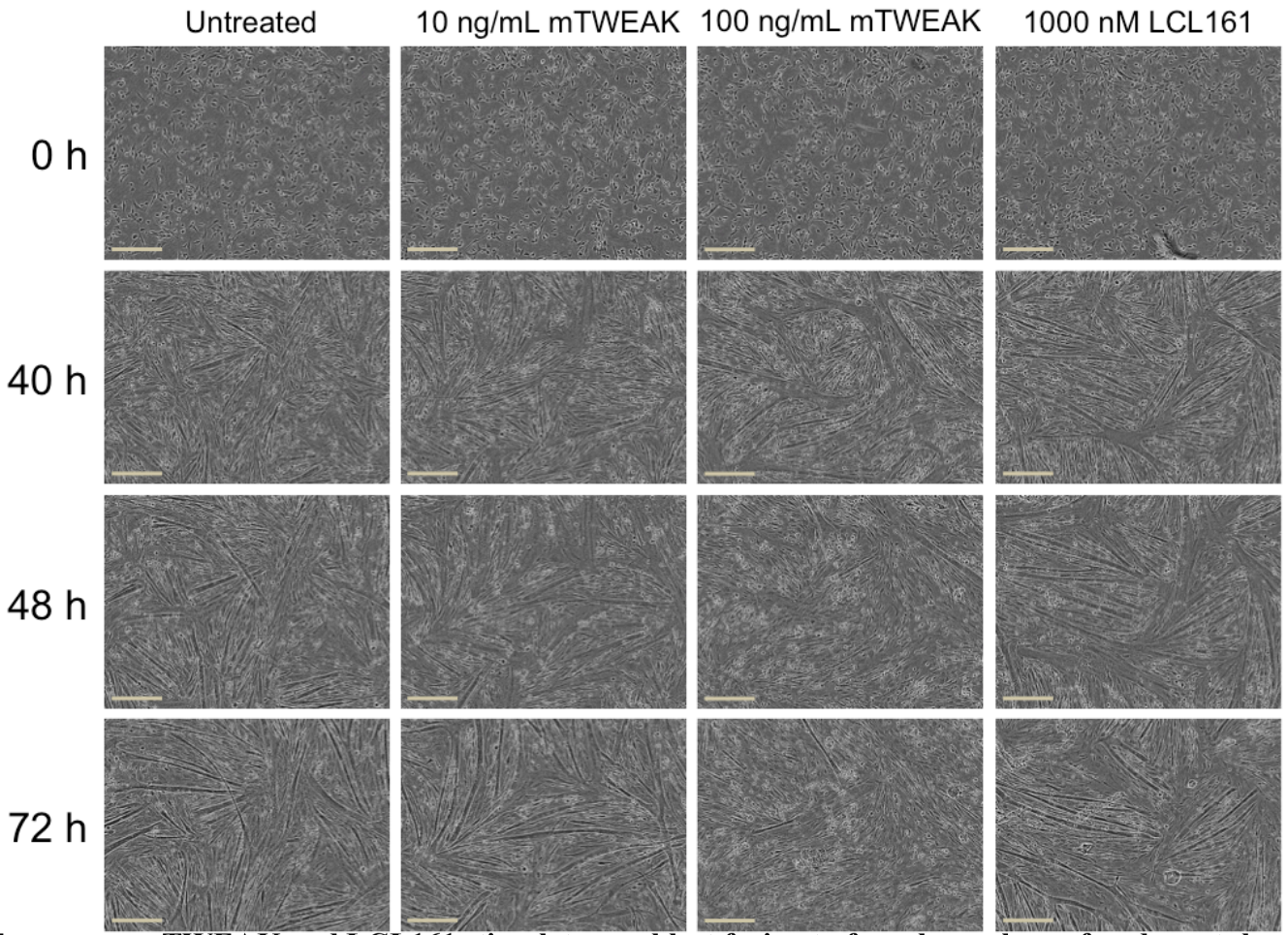

Fig. 10. Exogenous mTWEAK and LCL161 stimulate myoblast fusion to form large, hyperfused myotubes that shear off of tissue culture plates.

Phase contrast images of effect of low or high dose mTWEAK treatment or LCL161 treatment on wildtype primary myoblast differentiation. Cells were left to differentiate for a total of 72 hours. Images were obtained at 10X magnification via IncuCyte ZOOM® apparatus. Scale bar represents 300 μm. Experiment was repeated at least three times images represent one replicate.

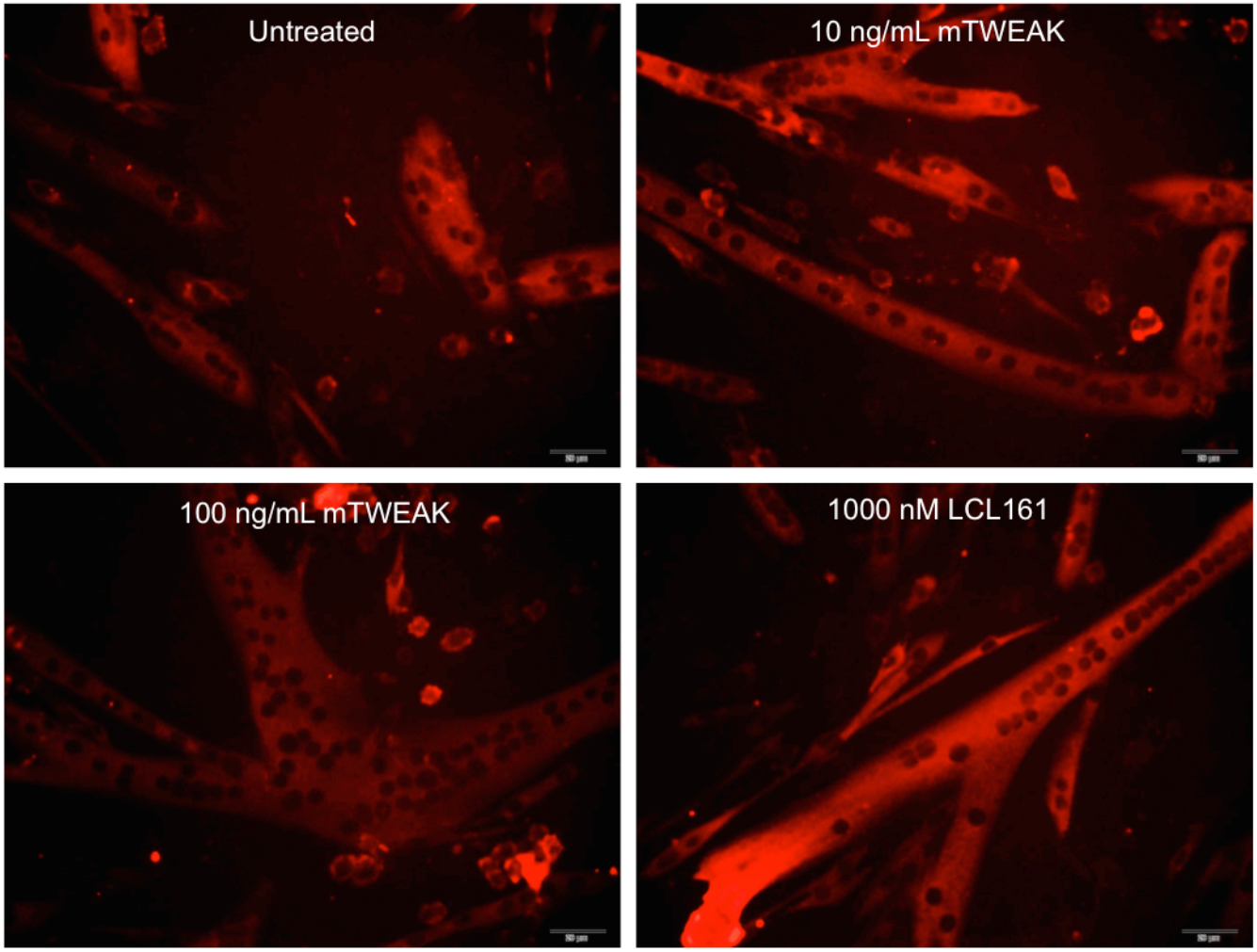

Fig. 11. Exogenous mTWEAK and LCL161 stimulate myoblast fusion to form large, hyperfused myotubes
Immunocytochemistry images targeting MHC to represent myotubes. Wildtype primary myoblasts were plated on coverslips, differentiated for 48 hours in differentiation media and fixed with 3.7% PFA prior to Fluorescent imaging. Experiment was repeated at least three times; images represent one replicate.

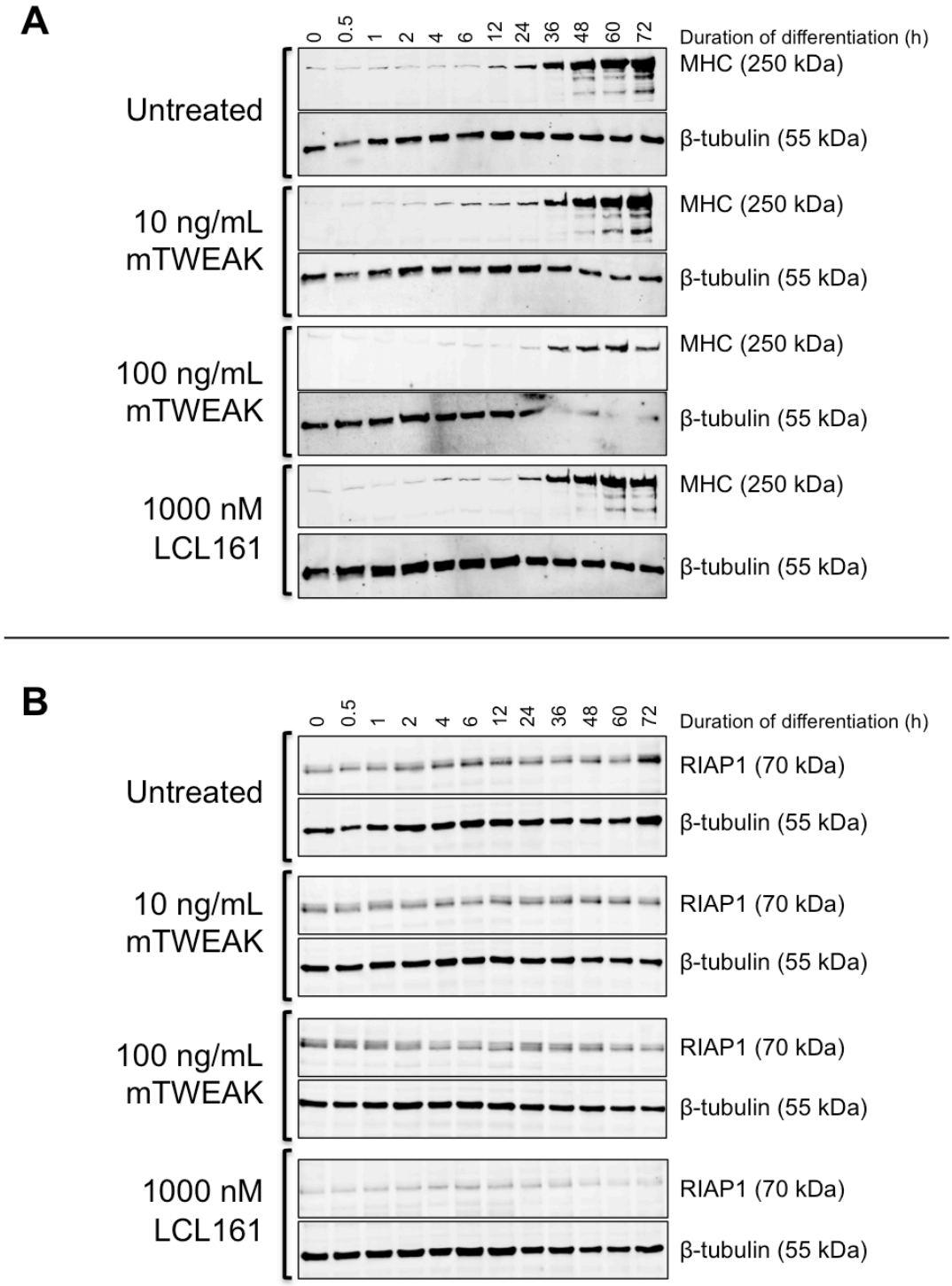

Fig. 12. Exogenous mTWEAK and LCL161 do not impact differentiation of myotubes; LCL161 and high doses of TWEAK lead to degradation of cIAP1.
Cell lysates were collected at designated timepoints and frozen until blotting. A: Myosin heavy chain (MHC) represents a marker of differentiation over the 72-hour differentiation period, with levels increasing as cells differentiate into myotubes. No significant differences are evident. 100 ng/mL TWEAK leads to shearing and thus inaccurate MHC detection. B: RIAP1 antibody is used to detect levels of both cIAP1 and cIAP2. Experiment was repeated at least three times; images represent one replicate.

leads to almost complete ablation of cIAP1 levels immediately upon treatment onset. Treatment with 100 ng/mL of mTWEAK led to a slight loss of cIAP1 as well, though this effect is much less rapid than that of the LCL161 treatment.

3.4 Exogenous mTWEAK triggers classical and alternative NF-κB signalling

The molecular mechanisms leading to the hyperfusion under conditions of exogenous mTWEAK and treatment with LCL161 were analyzed using protein lysates from the 72-hour differentiation period. Firstly, activation of the alternative NF-κB pathway was assessed using the proteolytic processing of p100 into p52. This was done through western blotting analysis of lysate samples, and is illustrated in **figure 13A**. In the untreated myoblasts, increased levels of p52 are evident within 2 hours of the onset of differentiation via incubation in low-serum differentiation media. However, this processing ceases by the end of the 72-hour period. Under low doses of mTWEAK, processing is more pronounced, though it only lasts up to 12 hours longer than the untreated conditions. In comparison, treatment with high doses of mTWEAK led to highly pronounced increases in levels of p52, starting within 2 hours of initiating differentiation, and only slightly decreasing by the end of analysis. Looking at the ratio of p52 levels to that of unprocessed p100, as shown in **figure 13B**, it is evident that proteolytic processing is markedly increased under all treatment conditions, though even more so for those of high doses of mTWEAK. A trend is seen with respect to reduction of processing by the end of the 72 hour incubation, though less so in the high dose treatment. Previous work with TWEAK noted that at low doses, signalling could activate the alternative pathway alone, but higher doses could activate the classical pathway

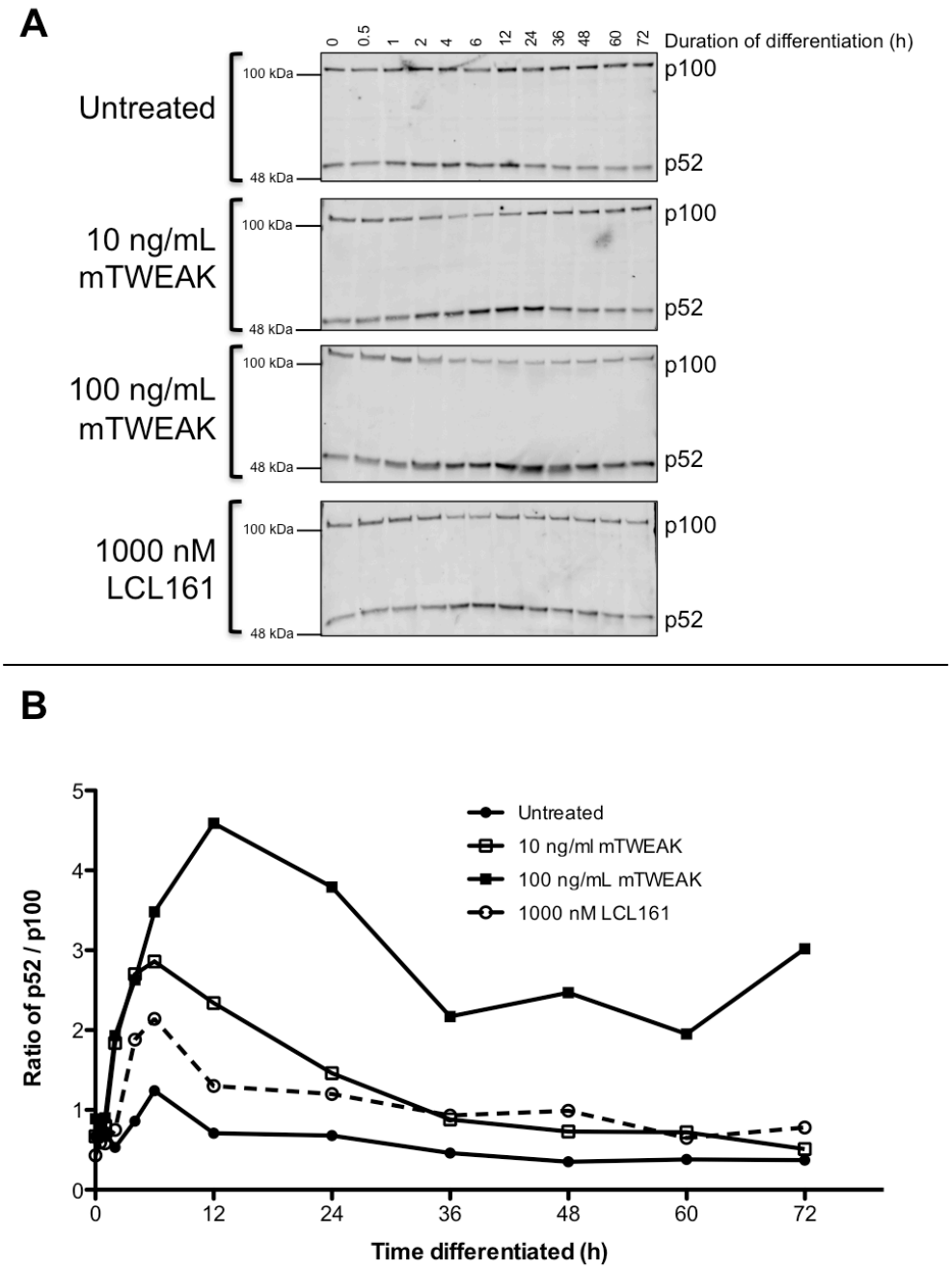

Fig. 13. mTWEAK and the SMC LCL161 activate alternative NF-κB signalling leading to p100 processing.

A: Western blotting analysis of wildtype myoblast differentiation showing levels of both unprocessed p100 and the processed form as p52. Significant processing is evident in both TWEAK treatments and that of LCL161. B: Densitometry analysis showing ratio of p52:p100, where a higher ratio indicates more robust processing, and thus increased alternative signalling. High levels of mTWEAK lead to significant processing.β-tubulin was used as a loading control, as shown in fig. 14. Experiment was repeated at least three times; images represent one replicate.

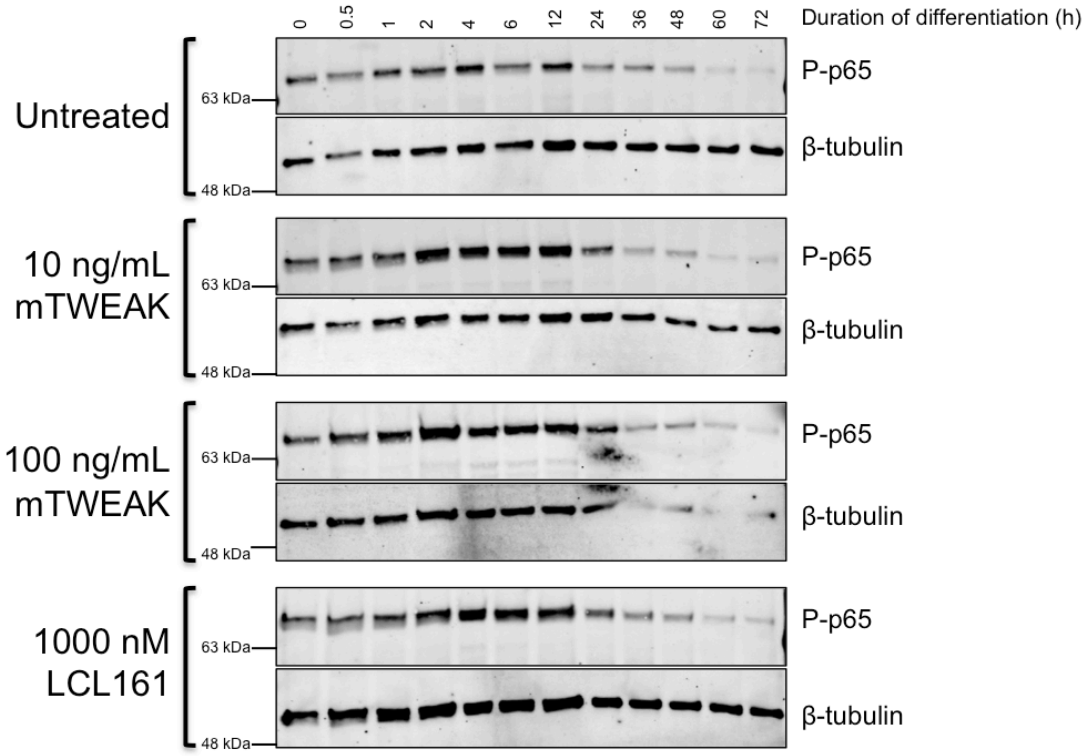

Fig. 14. mTWEAK and the SMC LCL161 activate classical NF-κB signalling through phosphorylation of p65; signalling is off by the end of the differentiation period. Western blotting analysis showing levels of phosphorylated p65, the more active form of the protein, in differentiating wildtype primary myoblasts over a 72-hour differentiation period. β-tubulin was used as a loading control. All three treatments activate classical signalling; signalling is off by the terminal differentiation point in all conditions. Experiment was repeated at least three times; images represent one replicate.

as well (Roos et al., 2010). Thus, the activation of the classical pathway was analyzed using protein lysates from the 72 hour differentiation period. This was done by western blot analysis of p65 (RelA) phosphorylation, and is shown in **figure 14**. In untreated myoblasts, phosphorylated p65 (P-p65) levels increase within 1 hour of switching to differentiation media, and decrease significantly starting at 24 hours into differentiation to very low levels by the 72-hour timepoint. Both low and high doses of mTWEAK, as well as the treatment with LCL161 resulted in an apparent increase in P-p65 levels in comparison to untreated control. Nevertheless, a decrease of P-p65 is evident between the 24 hour and 72 hour timepoints in all conditions.

3.5 Possible feedback loop of TWEAK and Fn14 expression following treatment with exogenous mTWEAK or LCL161

As mentioned in section 3.2, TWEAK mRNA was successfully detected in wildtype myoblasts, and was present for the duration of the differentiation process. Levels of TWEAK were thus more closely analyzed in the above 72-hour incubation experiment, with RNA extractions performed at similar timepoints for RT-qPCR analysis. In comparison to untreated controls, levels of TWEAK mRNA appears to decrease within 12 hours of treatment with exogenous mTWEAK at either concentration or with LCL161, but return to normal by the 72-hour timepoint. A similar decrease is observed in levels of Fn14 mRNA, though this response is more dose-dependent. Levels begin to increase again by the end of the 72-hour period for the low concentrations of exogenous mTWEAK and LCL161, but remain low throughout following treatment with high concentrations of mTWEAK.

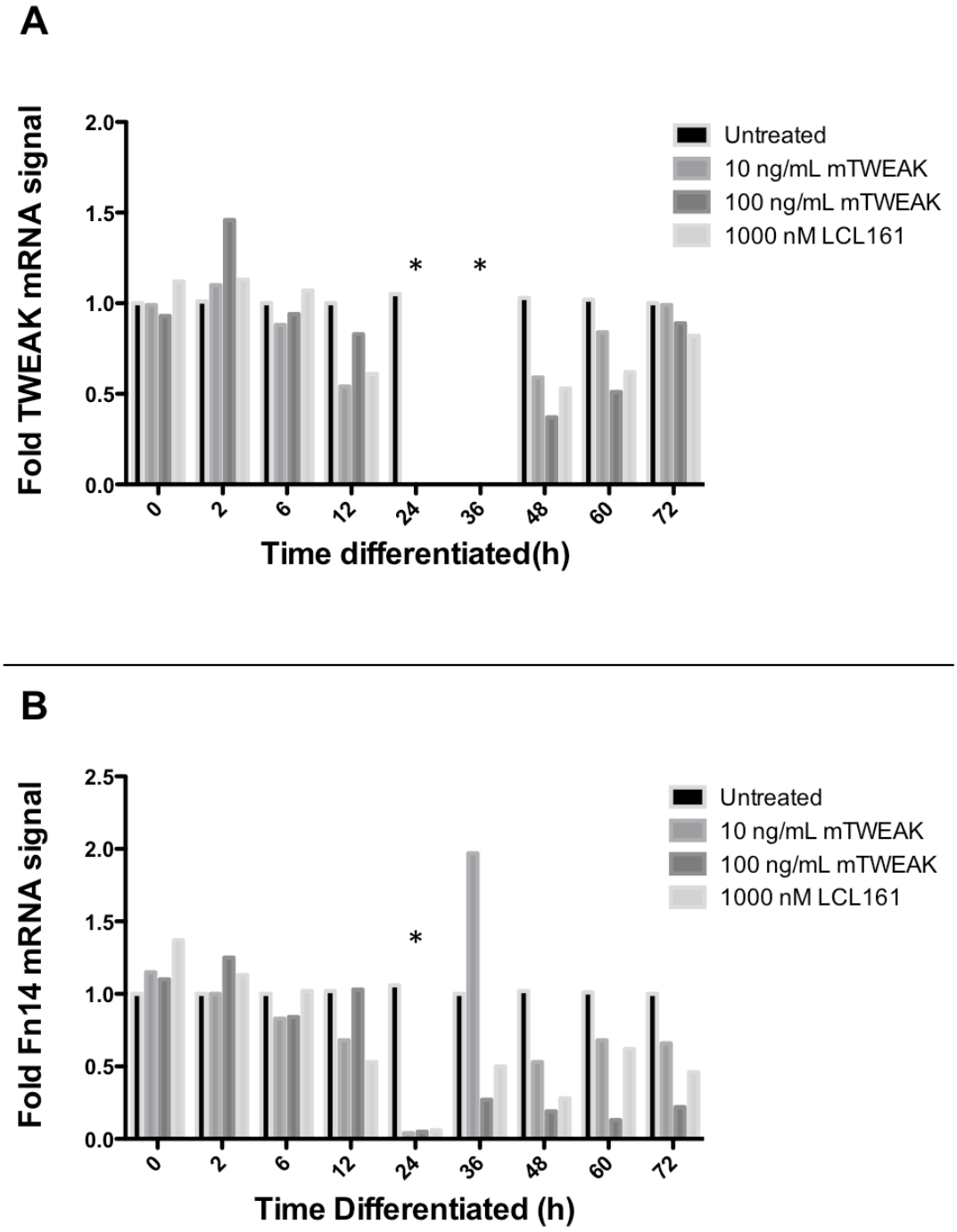

Fig. 15. A possible feedback loop of TWEAK and Fn14 expression exists following treatment with exogenous mTWEAK or LCL161.
RT-qPCR analysis of TWEAK and Fn14 mRNA over a 72-hour differentiation period of primary myoblasts was performed via RT-qPCR using Universal SYBR® Green Supermix reagents (Bio-Rad). B2M mRNA levels were used as a standardizing control. Levels between the treatment conditions were normalized to untreated control. Experiment was repeated at least three times; values represent one replicate. *indicates undetectable results due to technical error.

Chapter 4 – Discussion

4.1 In vitro 59-candidate low-throughput screen for factors involved in myoblast differentiation and fusion

Recent work in the field of muscle research has shown that the NF-κB signalling pathway plays a large role in myogenesis and muscle disease. Additional work has looked at the proteins cIAP1, TWEAK, and Fn14 with respect to their roles, specifically in terms of their own involvement in mediating the NF-κB pathway. Thus, a literature review of possible targets or mediators of NF-κB signalling and the myogenic process was performed, after which 59 targets were chosen for study. These included factors within the TNF superfamily such as TWEAK and TNF-α, the TNFRSF superfamily including Fn14 and TNFR1, their binding partners including TRAF2 and 3, the NF-κB members themselves such as p100 and IKKα, various other cytokines including IL4 and IL13, NFAT members including NFATc1-4 and NFAT5, bCatenin, Notch1 and 3 as well as targets of the Notch pathways, cell adhesion factors such as CD9 and CD36, cell motility factors including Rac1 and FAK, and miscellaneous factors including myomaker and c-Myb, all previously shown to play a role in some aspect of myoblast differentiation/fusion. A siRNA library for these 59 factors plus a non-targeting control was obtained from Dharmacon and used in a reverse transfection experiment to determine the impact of each protein on the process of myogenesis, as modeled in **figure 5.**

Previous reports have shown that primary myoblasts from cIAP1$^{-/-}$ mice display a hyperfusion phenotype following differentiation (Enwere et al., 2012). Thus, these myoblasts were used for the current study because scoring could be more robust given that the impact on the phenotype would be more drastic. After monitoring in the IncuCyte

ZOOM®, an incubator-housed fluorescent and phase contrast microscope, pictures of each well were scored based on the number of branch points in the image frame following optimal differentiation. More branch points on myotubes represent increased fusion, since they form due to the secondary fusion of myotubes with one another. Thus, the presence of less branch points in comparison to the non-targeting control (which contained an average of 18) could potentially indicate that the factor knocked down by the specific siRNA is involved in the fusion process. Those wells resulting in no branch points were assigned a score of -2, since secondary fusion was purportedly completely blocked. Wells showing 1-9 branch points were assigned a score of -1, since fusion was somewhat blocked though not completely. All targets whose knockdown resulted in 10-19 branch points were assigned a score of 0, since they were not drastically different than the control. Interestingly, knockdown of some targets resulted in increased fusion, showing the presence of many more branch points. These were assigned a score of +1 provided the number of branch points was above or equal to 20. Though admittedly open to bias, this scoring system allowed for the simple classification of the targets, and preliminary results suggested numerous targets to follow up on. It is important to note that the preliminary 59-candidate screen involved knockdown of targets via a combined pool of 4 unique siRNAs all targeting the same mRNA. Thus, it is possible that some scores are not representative of the true result of target knockdown, but instead are the result of an "off-target" effect, where a siRNA non-specifically targeted an unintended gene's mRNA.

However, the results as defined by this scoring system were nevertheless in line with the generally accepted roles of individual proteins in the differentiation and fusion processes. For example, previous worked looked at the impact of knocking down p100 and found that fusion was hindered due to blocking of the alternative NF-κB pathway. Since p100 must be

processed into p52 prior to nuclear translocation of the transcription factor, loss of p100 effectively blunts the alternative pathway. It is not surprising that knocking down NIK blocks the hyperfusion phenotype observed in cIAP1$^{-/-}$ myotubes. The alternative pathway is activated in these cells due to removal of cIAP1 since NIK is no longer targeted for degradation and is stabilized, and can then activate the proteolytic processing of p100 into p52. Thus, knockdown of NIK in these cIAP1$^{-/-}$ myoblasts effectively negates the fusion-promoting effects of cIAP1 loss on the differentiation process, and the hyperfusion phenotype is no longer observed.

The Notch family of proteins has received ample attention in the world of myogenesis, with recent works illustrating the vital role of the Notch pathway in the activation of satellite cells (Conboy and Rando, 2002; Conboy et al., 2003). One protein in the Notch family, DLL1, emerged as an interesting result in my 59-candidate screen. As illustrated in **figure 6,** loss of Delta1 or DLL1 in differentiating myoblasts resulted in a score of +1 due to the substantial amount of branch points present. In addition, the tubes formed were very large. This suggests that DLL1 inhibits the overall myogenic process, since its absence leads to hypertrophy of the tubes and an increase in fusion. In fact, previous work investigating the role of DLL1 in muscle pointed to its inhibitory effect on the myogenic process through preventing the myoblast to myocyte transition, and also through prevention of the specification of satellite cells to myoblasts (Schuster-Gossler et al., 2007).

Previous studies on the TNFRSF receptor Fn14 had also demonstrated that knockdown in myoblasts results in a complete loss of fusion (Dogra et al., 2007). Thus, my observed score of -2 is not surprising, and confirms these previous findings. Initially, the Fn14 binding partner TWEAK was included in the screen as a control of sorts, since it is generally accepted that myoblasts do not endogenously produce TWEAK, but instead just

respond to secreted TWEAK from other cells. However, the score of -1 from siTWEAK prompted further investigation, since this suggested that TWEAK is indeed endogenous to myoblasts, and moreover that it may have a significant role in the differentiation process. Thus, the role of TWEAK as an endogenous myokine was further investigated.

4.2 TWEAK is endogenous to myoblasts, and is involved in fusion

The TWEAK/Fn14 binding pair comprises a relatively novel signalling moiety in terms of their involvement in myogenesis, liver disease, and cancer. Although studies have shown the presence of the membrane-bound receptor Fn14 in myoblasts and in skeletal muscle in general, TWEAK was previously not thought to be endogenously expressed in muscle tissue or myoblasts. Thus, the fact that siRNA-mediated TWEAK knockdown caused an effect on the phenotype of terminally differentiated myoblasts constituted an interesting result. This finding was first followed up through verification of the presence of TWEAK mRNA within differentiating myoblasts. The mRNA was isolated at 24 hour intervals following the onset of differentiation through incubation in low-serum "differentiation media" (10% donor equine serum in DMEM). Using SYBRGreen RT-qPCR, TWEAK mRNA was found to be present within differentiating myoblasts for the duration of a 72-hour differentiation period, as illustrated in **figure 7**. This shows that TWEAK is produced by myoblasts and proposes a novel role for TWEAK. Although significant TWEAK expression has been shown in many different tissues including the heart, brain, and most notably skeletal muscle, no studies have previously shown endogenous expression by myoblasts specifically. Indeed, the current model, as proposed by previous studies, suggests that TWEAK is produced by and cleaved in infiltrating leukocytes within the muscle tissue. Though it has been shown through numerous studies that leukocytes do

indeed produce TWEAK, the results presented here pose a new model, illustrated in **figure 16**, in which TWEAK is endogenous to the myoblasts.

Once I had shown that TWEAK mRNA is present within the myoblasts, further work was done to investigate the effects of TWEAK knockdown therein on the differentiation process. The transfections were scaled up to a 6-well format to allow for the collection of both protein and mRNA from cells undergoing the siRNA-mediated knockdown and subsequent cell differentiation process. As mentioned in discussing the preliminary screen, some results as summarized in table 1 may be due to off-target effects rather than due to successful knockdown of the intended target protein. Thus, in doing a closer investigation of the role of TWEAK, each individual siRNA sequence was studied in conjunction with the siRNA pool to verify their results independently and as a set. In addition, the preliminary screen involved transfection of cIAP1$^{-/-}$ myoblasts in order for more robust differences in terminal differentiation phenotype to be evident. In further investigating TWEAK specifically, transfection experiments were repeated with wildtype (C57BL/6) myoblasts to further validate the results. The resulting phenotypes of each of these transfection reactions are shown in **figure 8**. These images illustrate the negative effects of TWEAK knockdown on myotube formation during the differentiation period. This is seen through the decreased number of myotubes present within those wells where TWEAK was targeted via siRNA transfection, and also to some extent through the apparent size of the tubes that did form.

In order to examine the effects of TWEAK knockdown at a more molecular level, western blotting was performed on protein lysates taken at 24-hour intervals over the course of differentiation. Myosin heavy chain (MHC) is commonly used as a marker of differentiation in both primary and immortalized myoblasts. In this experiment, as illustrated in **Figure 9A**, transfection with a non-targeting siRNA followed by a 72-hour differentiation

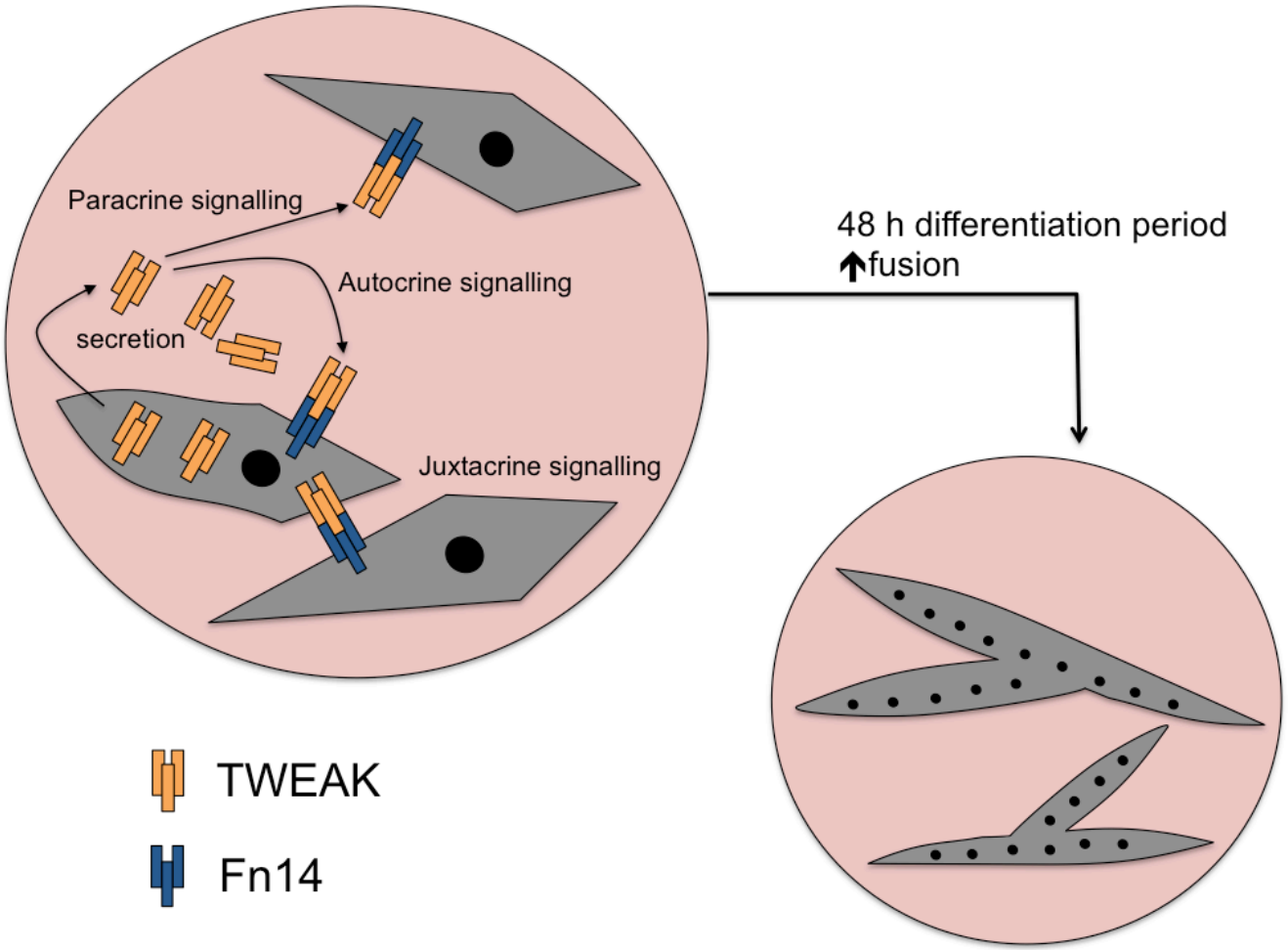

Fig. 16. Model of endogenous TWEAK production in myoblasts leading to signalling through Fn14 and increased fusion.

In vitro process is shown here, where TWEAK signalling through possible paracrine, autocrine, or juxtacrine signalling mechanisms leads to stimulation of fusion via activation of alternative NF-κB

period resulted in a gradual increase in MHC levels as differentiation occurred. When comparing the final MHC levels of each individual sample involving TWEAK knockdown to that of the non-targeting control, no significant difference was evident. This combined with the decrease in myotube branching suggests that it is fusion and not differentiation that is hindered by the loss of TWEAK. Myoblasts undergoing differentiation can fuse in one of two ways. Primary fusion involves that of individual mononuclear myoblasts with one another to form a binucleate cell. Secondary fusion involves the fusion of mononuclear myoblasts with nascent multinucleated tubes, forming larger tubes that may contain multiple branch points. My data thus suggests a role for TWEAK in the secondary fusion process, since myotubes did form but were small and unbranched. Furthermore, it also appears that following TWEAK knockdown, upregulation of MHC is delayed, as is differentiation due to the absence of TWEAK in differentiating cells. In order to verify the successful knockdown of TWEAK itself, RT-qPCR was performed on mRNA isolated from transfected primary myoblasts following the 24-hour transfection period. As illustrated in **figure 9B**, knockdown of TWEAK mRNA was successful in samples transfected with the pooled siRNA, as well as in samples transfected with deconvoluted siRNA #s 3 and 4.

4.3 Exogenous mTWEAK promotes myoblast fusion

Previous studies on TWEAK have suggested that this cytokine inhibits myoblast differentiation (Dogra et al., 2006; Girgenrath et al., 2006). However, a recent study from our lab proposed that inhibition only occurs at high concentrations of the protein (100 ng/mL or higher), while lower concentrations which are more representative of physiological levels (10 ng/mL) lead to increased fusion, resulting in a hyperfusion phenotype similar to that of cIAP1$^{-/-}$ myoblasts (Enwere et al., 2012). In order to more closely study this concentration-

dependent difference in phenotype, I repeated previously performed experiments (see Enwere et al., 2012) with equipment allowing for the microscopic visualization of the differentiation process at regular time intervals. This was done using the IncuCyte ZOOM® device and its accompanying software. The IncuCyte ZOOM® is a microscopic camera that can be configured to capture and save images of culture plates at desired timepoints, and is housed in a tissue culture incubator under standard conditions (37°C and 5% CO_2). C57BL/6 primary myoblasts were plated, incubated with differentiation media containing the appropriate concentration of exogenous murine TWEAK (mTWEAK), and monitored for a total of 72 hours. At first glance, the myotubes visualized at the final timepoint resembled those seen in the 2012 study in that a concentration of 100 ng/mL of mTWEAK seemingly inhibited myoblast differentiation and fusion, while the lower concentration of 10 ng/mL stimulated fusion to form large, hyperfused myotubes. However, using images captured every hour over the 72-hour differentiation period, I generated time-lapse videos for each individual well in order to visualize the entire length of the process. These videos show that the 100 ng/mL concentration of mTWEAK stimulates the process of fusion to such an extent that large, hyperfused myotubes form early, and are so large that they contract and shear off of the culture plates prematurely. Once the cells were no longer attached, the microscope camera was unable to visualize them, resulting in images of only the few remnant myoblasts. These myoblasts ultimately underwent differentiation as well, and since very few were present by this point, this resulted in the small myotubes with less branch points present at the final timepoint.

The hyperfused myotubes formed following treatment with exogenous mTWEAK closely resemble those formed by cIAP1$^{-/-}$ myoblasts, or those formed in wildtype myoblasts

receiving treatment with a SMC as represented in the previous study from our lab (Enwere et al., 2012). Thus, I wanted to compare the differentiation of myoblasts following treatment with exogenous mTWEAK with those following SMC treatment. Representative images of the differentiation process are shown in **figure 10**. Interestingly, the shearing effect observed when treating cells with high concentrations of mTWEAK is also seen following treatment with the SMC LCL161, though to a lesser extent. Immunocytochemistry images from experiments where MHC was labeled with red are shown in **figure 11.** These images further illustrate the robust fusion phenotype seen following treatment with 100 ng/mL mTWEAK, evident through the appearance of large multinucleated and branched tubes, which formed within 48 hours of differentiation. By this point, less robust fusion is evident following treatment with 10 ng/mL mTWEAK or 1000 nM LCL161. However, the phenotype observed following these two treatments still show more fusion relative to untreated control. Thus, it is clear that TWEAK signalling in myoblasts during differentiation leads to increased fusion. A similar effect is seen following treatment with the IAP antagonist drug LCL161.

In addition to studying the morphological phenotypes formed following these treatments, I investigate the effects of each treatment at the molecular level. Thus, I collected protein lysates at various timepoints over a 72-hour period for all treatment conditions. Treatment with a low concentration of mTWEAK did not impact myoblast differentiation, illustrated by the similarity in levels of MHC between that seen in the untreated control. Very low levels of MHC were detected in the conditions of high concentrations of mTWEAK in the remnant myoblasts/myotubes, though looking at levels of the loading control β-tubulin indicate that this may not be very representative. In addition,

protein lysates were collected through the scraping of adherent cells, meaning any myotubes that had previously detached due to shearing were not included in the western blotting analysis. No significant differences were detected following treatment with LCL161 either, although a delay in the increase of MHC levels was evident. Our lab previously observed this delay in differentiation following treatment with a SMC (Enwere et al., 2012). These results once more suggests a role for TWEAK and furthermore for loss of cIAP1 specifically in the process of fusion, since differentiation itself is seemingly unaffected. A more thorough discussion of the molecular effects of each treatment condition follows below, in section 4.4.

Lastly, in order to verify that loss of cIAP1/2 occurred via treatment with SMC, blotting was performed using the RIAP1 antibody, as validated by previous work (Holcik et al., 2002). As illustrated in **figure 12B**, SMC treatment causes complete loss of cIAP1/2, indicating effective activity of the drug. SMCs are small molecules that mimic the activities of the Smac protein, which antagonizes the IAPs by binding to their BIR domain. Specifically in the case of the cIAPs, this binding causes auto-ubiquitination of both cIAP1 and cIAP2, leading to their proteasome-mediated degradation (Varfolomeev et al., 2007; Vince et al., 2007). SMC molecules are designed to mimic the N-terminal tetrapeptide AVPI sequence of processed Smac, conferring upon them their binding capabilities. Interestingly, treatment with high concentrations of mTWEAK seemingly decreased levels of cIAP1 as well, though not to the extent seen following LCL161 treatment. This phenomenon has been reported in previous studies, where treatment of cells with TWEAK led to decreased levels of intracellular cIAP1 due to proteasomal degradation (Varfolomeev et al., 2007; Vince et al., 2008). This degradation occurs following sequestration of cIAP1 to a membrane

complex along with TRAF2, TRAF3, and Fn14. The signalling ramifications of loss of cIAP1/2 on myogenesis will be discussed further below.

4.4 Exogenous mTWEAK, LCL161 triggers both classical and alternative NF-κB signalling

Much time and effort has been dedicated over the years to studying the NF-κB pathway and its downstream signalling. Recent studies have demonstrated that TWEAK and its receptor Fn14 activate this ubiquitous signalling pathway, though activation is dose-dependent with respect to the strength of the signalling response as well as the nature of the response. Two distinct arms of NF-κB signalling exist, namely the classical and alternative pathways. Using protein lysates from the 12 timepoints mentioned above, I analyzed the signalling response that occurs following treatment with low concentrations (10 ng/mL) and high concentrations (100 ng/mL) of mTWEAK, as well as 1000 nM LCL161 in comparison to an untreated control. First, p100 processing into p52 was used as a marker for activation of the alternative NF-κB pathway. As shown in **figure 13A**, in untreated myoblasts levels of p100 remain fairly constant throughout the differentiation process. However, an increase in p52 levels is seen within 2 hours of the onset of differentiation. This spike dissipates by the 24-hour timepoint, with p52 levels remaining consistently low until the termination of differentiation. Following treatment with low concentrations of mTWEAK, a more significant increase in p52 levels is evident by the second hour of differentiation in comparison to the untreated control, and levels remain high for at least 12 more hours. A noticeable decrease in p100 levels is also detectable within the same time range. As would be expected of a dose-dependent response, treatment with high concentrations of mTWEAK

led to an even more robust increase in p52 levels within two hours of the start of differentiation. Interestingly, these remain elevated for the duration of the 72-hour differentiation. This corresponds to a noted decrease in levels of p100 evident for the same time period. Treatment with LCL161 mimics that of treatment with low concentrations of mTWEAK, where p52 levels increased between the 2-24 hour periods but returned to baseline for the remainder of the differentiation period. Although these qualitative findings are significant, a more quantitative approach to studying p100 processing rests in the ratio of p52 to p100. A large ratio suggests the cell is actively working to process p100 into p52 at a rate faster than the production of p100, thereby indicating activation of the alternative NF-κB pathway. Using the blots, I performed a densitometric analysis to analyze this ratio. As illustrated in **figure 13B** and as suggested by the qualitative analysis of the blots, treatment with high levels of exogenous mTWEAK led to high, sustained rates of p100 processing. Treatment with lower doses also led to significant processing, though this effect tapered off by the 36 hour timepoint. Treatment with LCL161 mimics that seen in low-dose mTWEAK conditions, though to a lesser extent. Of note, a rapid increase in processing is observed for all conditions between the 1-4 hour marks, including the untreated control. These results indicate that treatment with 100 ng/mL of exogenous mTWEAK causes robust, prolonged activation of the alternative pathway, while a dose of 10 ng/mL causes less robust, transient activation thereof. A model representing the mechanisms behind TWEAK-mediated activation of the alternative NF-κB pathway is illustrated in **figure 4**. Treatment with LCL161 also causes transient alternative NF-κB activation, through degradation of cIAP1.

Previous studies on TWEAK have shown that the cytokine can also activate classical NF-κB signalling at certain doses. Thus, using phosphorylated p65 (P-p65) as a marker of

classical NF-κB signalling activation, I compared this signalling response in the four treatment conditions. In the untreated control, P-p65 levels increased slightly within one hour of the onset of differentiation, followed by a rapid decrease by the 24-hour mark. Levels remained low for the remainder of the differentiation process. All three other treatment conditions resulted in substantial increases in P-p65 levels within one hour of the onset of differentiation, with levels drastically decreasing starting at the 36 hour timepoint and throughout the remainder of the differentiation process. Thus, treatment with exogenous mTWEAK or LCL161 caused a slight delay in the usual decrease of classical NF-κB signalling during differentiation.

Based upon the results of previous studies on the NF-κB pathways and myogenesis, the two separate arms of the pathways are proposed to play unique yet paradoxically interlinked roles. Classical NF-κB signalling in myoblasts has been linked to increased proliferation, as discussed in section 1.3. More importantly, it has been linked to the inhibition of the differentiation process both through stimulating the G1/S cell cycle transition and through degradation of MyoD mRNA (Dahlman et al., 2009; Guttridge et al., 1999, 2000). The less-studied alternative NF-κB pathway has been linked with stimulating myoblast differentiation and fusion and in myotube maintenance. Activation thereof through loss of cIAP1 has been shown to lead to increased fusion resulting in large, multinucleated myofibres (Enwere et al., 2012). In fact, one study showed that overexpression of NIK leads to increased fusion in differentiating myoblasts (Canicio et al., 2001). Previous work has also suggested that the alternative NF-κB pathway is highly involved in myotube homeostasis and mitochondrial biogenesis (Bakkar et al., 2008). Thus, as illustrated in **figure 3**, a model representing the relationship between the two pathways in the transition

from myoblasts to myotubes was recently proposed, where classical signalling is active in proliferating myoblasts, and must be terminated for proper differentiation to occur. This termination is closely linked with activation of alternative NF-κB signalling, which is highly active during differentiation. My results closely recapitulate results from these previous studies. The classical NF-κB pathway, represented by levels of P-p65, is active in the myoblasts for the first few hours following the switch to differentiation media. During this time, little differentiation occurs, as the classical pathway is still active and the myoblasts keep proliferating. The classical pathway is clearly triggered to stop signalling by the 24-hour timepoint, as levels of P-p65 diminish drastically thereafter. In fact, decreases can be noted as early as 12 hours into differentiation. This roughly coincides with the point at which alternative signalling is most active, represented by large ratios of p52:p100, which indicate significant processing of p100 into p52. It is interesting to note that slightly lower levels of MHC at the 24-hour timepoint within both mTWEAK treatment conditions as well as following treatment with LCL161 are apparent in comparison with the untreated control. This coincides with slightly higher levels of P-p65, illustrating the inhibitory effects of the classical pathway on the differentiation process. The robust, sustained activation of the alternative NF-κB signalling pathway following treatment with high concentrations of mTWEAK can be linked to the hyperfusion phenotype observed by the 40-hour mark, as illustrated in **figure 10**. Alternative NF-κB signalling has been previously linked to such a phenotype (Enwere et al., 2012), and in my experiment hyperactive signalling amplified this effect to the point where the formed myotubes contracted, shearing off of the culture plates at early time points. The remaining cells still exhibited high levels of alternative NF-κB signalling, resulting in the second round of fusion evident in the attached video starting at

day 2 13:00. It must be noted that a 2010 study by Roos *et al.* looking at the dose-dependent effects of TWEAK showed that low levels such as 10 ng/mL were not able to activate the classical NF-κB pathway, while high levels such as 100 ng/mL activated both arms of the NF-κB pathway. This study looked at the molecular nature of the secreted TWEAK molecules, specifically with respect to whether they existed as a trimer or an oligomer. With respect to this feature of TWEAK signalling, it was found that while trimeric binding only activated the alternative pathway, oligomeric TWEAK activated both classical and alternative signalling. Of note, the authors mention that mTWEAK generated in bacteria, such as that used in this experiment, likely exists in an oligomeric form, and thus signals more strongly than endogenously produced murine TWEAK moieties (Roos et al., 2010).

4.5 Possible feedback loop of TWEAK and Fn14 expression following treatment with exogenous mTWEAK or LCL161

In order to further investigate the endogenous nature of TWEAK within differentiating myoblasts, I isolated mRNA from a range of timepoints over the course of a 72-hour differentiation period for analysis via RT-qPCR. TWEAK message levels were measured using B2M as a normalizing control. Message levels in each treatment condition were compared to that of the untreated condition. The results graphed in **figure 15A** illustrate that treatment with exogenous TWEAK seemingly causes a decrease in TWEAK mRNA production within 12 hours of incubation. These levels return to 'baseline' levels by the end of the 72-hour period. This suggests that an autocrine feedback loop exists within the myoblasts, where high levels of TWEAK within the media signal to slow endogenous TWEAK production within the cells. Interestingly, treatment with LCL161 causes a similar

decrease in TWEAK mRNA levels, indicating that loss of cIAP1/2 within the myoblasts may be a key factor in regulating TWEAK production. A recently proposed model suggests that TWEAK activates alternative NF-κB signalling through sequestration of cIAP1/2 to a membrane-bound protein complex, effectively blocking their usual repressive ubiquitination of NIK (Enwere et al., 2014). Thus, high levels of exogenous TWEAK that stimulate this sequestration function may cause the cell to slow endogenous TWEAK production, and a similar effect could be elicited by removal of cIAP1/2 through SMC treatment. I also analyzed message levels of the membrane-bound receptor Fn14. As shown in **figure 15B**, a similar decrease in Fn14 mRNA levels is seen in response to treatment with exogenous mTWEAK or LCL161. This effect is much larger when concentrations of exogenous mTWEAK are higher. Unlike TWEAK mRNA levels, production of Fn14 mRNA does not return to baseline levels by the end of the 72-hour period. My data support the idea of an autocrine feedback loop in response to exogenous levels of TWEAK protein. It is important to note that while my data suggest an autocrine loop at the level of transcription, they may not correlate with the rate of mRNA translation, protein stability or excretion for example. Thus, levels of TWEAK or Fn14 protein may not be affected despite a reduction in the rate of transcription. Further analysis must be performed in order to determine whether protein levels themselves are altered, either by western blotting or ELISA.

4.6 The compounding data surrounding TWEAK/Fn14 activity

Many groups have studied the role of the TWEAK/Fn14 pair within skeletal muscle, which has resulted in some confounding data. Numerous papers have reported negative effects of TWEAK within skeletal muscle. One study showed almost complete inhibition of

differentiation in both primary myoblasts and C2C12 myoblasts following incubation with exogenous TWEAK (Dogra et al., 2006). However, it must be noted that these experiments involved TWEAK levels five times the maximum dose used in my experiments. It is thus possible that under these conditions, classical NF-κB activation is so robust that proliferation is pathologically activated, thus inhibiting the differentiation process entirely. Much work has also been done with respect to genetic modifications of TWEAK expression. TWEAK knockout (TWEAK-KO) mice show no overt phenotype in skeletal muscle, and are structurally identical to wildtype mice at 3 months of age. In contrast, transgenic TWEAK mice (TWEAK-Tg) exhibiting four- to six-fold increases in TWEAK expression show significant muscle atrophy and fibrosis by 6 months of age (Mittal et al., 2010b). Using these mice, it was shown that by 10-21 days following cardiotoxin injection, TWEAK-KO mice exhibited larger myofibres in comparison to wildtype controls. The opposite effect was seen in TWEAK-Tg mice, where regenerated fibres were significantly smaller. In looking at nucleation of the regenerated fibres, the authors noted increased and decreased multinucleation of fibres in TWEAK-KO mice and TWEAK-Tg mice respectively, and suggested that TWEAK interferes with fusion during muscle repair (Mittal et al., 2010a). Though this seems contradictory to my results, it must be noted that no differences in fibre size were detectable 5 days post-CTX injection; differences only became evident after day 10, at which point multinucleation was measured as well. Similarly, recent work has suggested that concentrations of TWEAK close to physiological levels are beneficial for the differentiation process, while significantly higher levels may be pathological (Enwere et al., 2012). In the TWEAK-Tg mice, a four- to six-fold increase in TWEAK levels compared to wildtype controls may in fact represent these pathological effects. The cardiotoxin model

has also been used by two separate groups to study TWEAK and Fn14 expression in muscle following injury. Under these conditions, expression of TWEAK and Fn14 were shown to be increased at both the mRNA and protein levels following muscle injury (Girgenrath et al., 2006; Mittal et al., 2010a). One group further showed that $Fn14^{-/-}$ mice showed significant delays in regeneration as marked by the decreased amount of centrally nucleated fibres as well as delayed clearance of inflammation. Moreover, a drastic increase in TWEAK levels was detected in both control mice and $Fn14^{-/-}$ mice 3 days post-injury; these levels returned to baseline levels by day 5 in control mice, but remained high in $Fn14^{-/-}$ mice (Girgenrath et al., 2006). The authors suggest that the regenerative delay is likely due to a loss of sufficient myoblast proliferation because of a decrease in TWEAK signalling, though it is possible that an inhibition of fusion further adds to the delay. In 2010, a study looked at the role of TWEAK within skeletal muscle atrophy using TWEAK-KO mice in comparison with TWEAK-Tg mice. TWEAK-KO mice exhibited increased levels of Fn14 mRNA in comparison with control mice, as well as to TWEAK-Tg mice, who showed no difference from controls. Upon muscle denervation, a common model for atrophy due to immobilization and lack of neural input, wildtype C57BL/6 mice exhibited increased muscular levels of Fn14 mRNA and protein (Mittal et al., 2010b).

4.7 Conclusions and future directions

My data in conjunction with previously reported data supports the notion that TWEAK is involved in myoblast fusion. As I showed through siRNA-mediated knockdown, the loss of TWEAK did not impact differentiation but led to a significant decrease in secondary fusion resulting in thin, unbranched myotubes. I also showed, for the first time, that TWEAK is an endogenous factor produced by myoblasts, which promotes cell fusion.

Furthermore, I confirmed that incubation with exogenous mTWEAK led to increased fusion within differentiating myoblasts, as previously found by our lab (Enwere et al., 2012). At higher concentrations, this effect was large enough to cause *in vitro* myotube contraction, leading to the cells shearing off of the culture plates. Through molecular analysis, I have shown that TWEAK and LCL161 activate both the classical and alternative NF-κB pathways, though classical NF-κB signalling is subsequently drastically decreased early within the process. I thus propose that TWEAK signals to activate myoblast fusion through robust activation of alternative NF-κB signalling. I have also shown that a possible feedback loop exists within myoblasts to regulate endogenous production of both TWEAK and Fn14 in response to exogenous levels of TWEAK. TWEAK and Fn14 thus emerge as possible therapeutic targets for the treatment of muscle disease and for the repair of muscle injury.

References

Acharyya, S., Butchbach, M.E.R., Sahenk, Z., Wang, H., Saji, M., Carathers, M., Ringel, M.D., Skipworth, R.J.E., Fearon, K.C.H., Hollingsworth, M.A., et al. (2005). Dystrophin glycoprotein complex dysfunction: a regulatory link between muscular dystrophy and cancer cachexia. Cancer Cell *8*, 421–432.

Acharyya, S., Villalta, S.A., Bakkar, N., Bupha-Intr, T., Janssen, P.M.L., Carathers, M., Li, Z.-W., Beg, A.A., Ghosh, S., Sahenk, Z., et al. (2007). Interplay of IKK/NF-kappaB signaling in macrophages and myofibers promotes muscle degeneration in Duchenne muscular dystrophy. J. Clin. Invest. *117*, 889–901.

Anker, S.D., and Coats, A.J. (1998). Cachexia in heart failure is bad for you. Eur. Heart J. *19*, 191–193.

Bakkar, N., Wang, J., Ladner, K.J., Wang, H., Dahlman, J.M., Carathers, M., Acharyya, S., Rudnicki, M.A., Hollenbach, A.D., and Guttridge, D.C. (2008). IKK/NF-kappaB regulates skeletal myogenesis via a signaling switch to inhibit differentiation and promote mitochondrial biogenesis. J. Cell Biol. *180*, 787–802.

Bankolé, L.-C., Feasson, L., Ponsot, E., and Kadi, F. (2013). Fibre type-specific satellite cell content in two models of muscle disease. Histopathology *63*, 826–832.

Birnbaum, M.J., Clem, R.J., and Miller, L.K. (1994). An apoptosis-inhibiting gene from a nuclear polyhedrosis virus encoding a polypeptide with Cys/His sequence motifs. J. Virol. *68*, 2521–2528.

Boldrin, L., Zammit, P.S., and Morgan, J.E. (2015). Satellite cells from dystrophic muscle retain regenerative capacity. Stem Cell Res. *14*, 20–29.

Bossen, C., Ingold, K., Tardivel, A., Bodmer, J.-L., Gaide, O., Hertig, S., Ambrose, C., Tschopp, J., and Schneider, P. (2006). Interactions of tumor necrosis factor (TNF) and TNF receptor family members in the mouse and human. J. Biol. Chem. *281*, 13964–13971.

Bover, L.C., Cardó-Vila, M., Kuniyasu, A., Sun, J., Rangel, R., Takeya, M., Aggarwal, B.B., Arap, W., and Pasqualini, R. (2007). A previously unrecognized protein-protein interaction between TWEAK and CD163: potential biological implications. J. Immunol. *178*, 8183–8194.

Braun, T., Buschhausen-Denker, G., Bober, E., Tannich, E., and Arnold, H.H. (1989). A novel human muscle factor related to but distinct from MyoD1 induces myogenic conversion in 10T1/2 fibroblasts. EMBO J. *8*, 701–709.

Braun, T., Bober, E., Winter, B., Rosenthal, N., and Arnold, H.H. (1990). Myf-6, a new member of the human gene family of myogenic determination factors: evidence for a gene cluster on chromosome 12. EMBO J. *9*, 821–831.

Brown, S.A.N., Richards, C.M., Hanscom, H.N., Feng, S.-L.Y., and Winkles, J.A. (2003). The Fn14 cytoplasmic tail binds tumour-necrosis-factor-receptor-associated factors 1, 2, 3 and 5 and mediates nuclear factor-kappaB activation. Biochem. J. *371*, 395–403.

Brown, S.A.N., Ghosh, A., and Winkles, J.A. (2010). Full-length, membrane-anchored TWEAK can function as a juxtacrine signaling molecule and activate the NF-kappaB pathway. J. Biol. Chem. *285*, 17432–17441.

Brown, S.A.N., Cheng, E., Williams, M.S., and Winkles, J.A. (2013). TWEAK-independent Fn14 self-association and NF-κB activation is mediated by the C-terminal region of the Fn14 cytoplasmic domain. PLoS One *8*, e65248.

Cai, D., Frantz, J.D., Tawa, N.E., Melendez, P.A., Oh, B.-C., Lidov, H.G.W., Hasselgren, P.-O., Frontera, W.R., Lee, J., Glass, D.J., et al. (2004). IKKbeta/NF-kappaB activation causes severe muscle wasting in mice. Cell *119*, 285–298.

Canicio, J., Ruiz-Lozano, P., Carrasco, M., Palacin, M., Chien, K., Zorzano, A., and Kaliman, P. (2001). Nuclear Factor B-inducing Kinase and I B Kinase- Signal Skeletal Muscle Cell Differentiation. J. Biol. Chem. *276*, 20228–20233.

Carmeli, E., Coleman, R., and Reznick, A.Z. (2002). The biochemistry of aging muscle. Exp. Gerontol. *37*, 477–489.

Chicheportiche, Y., Bourdon, P.R., Xu, H., Hsu, Y.M., Scott, H., Hession, C., Garcia, I., and Browning, J.L. (1997). TWEAK, a new secreted ligand in the tumor necrosis factor family that weakly induces apoptosis. J. Biol. Chem. *272*, 32401–32410.

Collart, M. a, Baeuerle, P., and Vassalli, P. (1990). Regulation of tumor necrosis factor alpha transcription in macrophages: involvement of four kappa B-like motifs and of constitutive and inducible forms of NF-kappa B. Mol. Cell. Biol. *10*, 1498–1506.

Collins, C.A., Olsen, I., Zammit, P.S., Heslop, L., Petrie, A., Partridge, T.A., and Morgan, J.E. (2005). Stem cell function, self-renewal, and behavioral heterogeneity of cells from the adult muscle satellite cell niche. Cell *122*, 289–301.

Conboy, I.M., and Rando, T.A. (2002). The Regulation of Notch Signaling Controls Satellite Cell Activation and Cell Fate Determination in Postnatal Myogenesis. Dev. Cell *3*, 397–409.

Conboy, I.M., Conboy, M.J., Smythe, G.M., and Rando, T.A. (2003). Notch-mediated restoration of regenerative potential to aged muscle. Science *302*, 1575–1577.

Conze, D.B., Albert, L., Ferrick, D.A., Goeddel, D. V, Yeh, W.-C., Mak, T., and Ashwell, J.D. (2005). Posttranscriptional downregulation of c-IAP2 by the ubiquitin protein ligase c-IAP1 in vivo. Mol. Cell. Biol. *25*, 3348–3356.

Cornelison, D.D., and Wold, B.J. (1997). Single-cell analysis of regulatory gene expression in quiescent and activated mouse skeletal muscle satellite cells. Dev. Biol. *191*, 270–283.

Crook, N.E., Clem, R.J., and Miller, L.K. (1993). An apoptosis-inhibiting baculovirus gene with a zinc finger-like motif. J. Virol. *67*, 2168–2174.

Dahlman, J.M., Wang, J., Bakkar, N., and Guttridge, D.C. (2009). The RelA/p65 subunit of NF-kappaB specifically regulates cyclin D1 protein stability: implications for cell cycle withdrawal and skeletal myogenesis. J. Cell. Biochem. *106*, 42–51.

Davis, R.L., Weintraub, H., and Lassar, A.B. (1987). Expression of a single transfected cDNA converts fibroblasts to myoblasts. Cell *51*, 987–1000.

Dogra, C., Changotra, H., Mohan, S., and Kumar, A. (2006). Tumor necrosis factor-like weak inducer of apoptosis inhibits skeletal myogenesis through sustained activation of nuclear factor-kappaB and degradation of MyoD protein. J. Biol. Chem. *281*, 10327–10336.

Dogra, C., Hall, S.L., Wedhas, N., Linkhart, T. a., and Kumar, A. (2007). Fibroblast growth factor inducible 14 (Fn14) is required for the expression of myogenic regulatory factors and differentiation of myoblasts into myotubes: Evidence for tweak-independent functions of Fn14 during myogenesis. J. Biol. Chem. *282*, 15000–15010.

Edmondson, D.G., and Olson, E.N. (1989). A gene with homology to the myc similarity region of MyoD1 is expressed during myogenesis and is sufficient to activate the muscle differentiation program. Genes Dev. *3*, 628–640.

Enwere, E.K., Holbrook, J., Lejmi-Mrad, R., Vineham, J., Timusk, K., Sivaraj, B., Isaac, M., Uehling, D., Al-awar, R., LaCasse, E., et al. (2012). TWEAK and cIAP1 Regulate Myoblast Fusion Through the Noncanonical NF- B Signaling Pathway. Sci. Signal. *5*, ra75–ra75.

Enwere, E.K., LaCasse, E.C., Adam, N.J., and Korneluk, R.G. (2014). Role of the TWEAK-Fn14-cIAP1-NF-??B signaling axis in the regulation of myogenesis and muscle homeostasis. Front. Immunol. *5*, 1–13.

Evans, W.J. (1995). What Is Sarcopenia? Journals Gerontol. Ser. A Biol. Sci. Med. Sci. *50A*, 5–8.

Evans, W.J., and Wayne, A. (1993). Advances and Physiological Interrelationships Sarcopenia and Age-Related Changes in Body Composition and Functional Capacity1. Nutr. Res. 465–468.

Evans, W.K., Makuch, R., Clamon, G.H., Feld, R., Weiner, R.S., Moran, E., Blum, R., Shepherd, F.A., Jeejeebhoy, K.N., and DeWys, W.D. (1985). Limited impact of total parenteral nutrition on nutritional status during treatment for small cell lung cancer. Cancer Res. *45*, 3347–3353.

Fearon, K.C., Voss, A.C., Hustead, D.S., and for the Cancer Cachexia Study Group (2006). Definition of cancer cachexia: effect of weight loss, reduced food intake, and systemic inflammation on functional status and prognosis. Am J Clin Nutr *83*, 1345–1350.

Feng, S.L., Guo, Y., Factor, V.M., Thorgeirsson, S.S., Bell, D.W., Testa, J.R., Peifley, K.A., and Winkles, J.A. (2000). The Fn14 immediate-early response gene is induced during liver regeneration and highly expressed in both human and murine hepatocellular carcinomas. Am. J. Pathol. *156*, 1253–1261.

Forbes, G.B., and Reina, J.C. (1970). Adult lean body mass declines with age: some longitudinal observations. Metabolism. *19*, 653–663.

Girgenrath, M., Weng, S., Kostek, C.A., Browning, B., Wang, M., Brown, S.A.N., Winkles, J.A., Michaelson, J.S., Allaire, N., Schneider, P., et al. (2006). TWEAK, via its receptor Fn14, is a novel regulator of mesenchymal progenitor cells and skeletal muscle regeneration. EMBO J. *25*, 5826–5839.

Grounds, M.D. (1998). Age-associated changes in the response of skeletal muscle cells to exercise and regeneration. Ann. N. Y. Acad. Sci. *854*, 78–91.

Guttridge, D.C., Albanese, C., Reuther, J.Y., Pestell, R.G., and Baldwin, A.S. (1999). NF-kappaB controls cell growth and differentiation through transcriptional regulation of cyclin D1. Mol. Cell. Biol. *19*, 5785–5799.

Guttridge, D.C., Mayo, M.W., Madrid, L. V, Wang, C.Y., and Baldwin, A.S. (2000). NF-kappaB-induced loss of MyoD messenger RNA: possible role in muscle decay and cachexia. Science *289*, 2363–2366.

Haimes, J., Kelley, M., and Scientific, T.F. (2010). Demonstration of a ΔΔ C q Calculation Method to Compute Relative Gene Expression from qPCR Data. 1–4.

Hinds, M.G., Norton, R.S., Vaux, D.L., and Day, C.L. (1999). Solution structure of a baculoviral inhibitor of apoptosis (IAP) repeat. Nat. Struct. Biol. *6*, 648–651.

Hinz, M., Lemke, P., Anagnostopoulos, I., Hacker, C., Krappmann, D., Mathas, S., Dörken, B., Zenke, M., Stein, H., and Scheidereit, C. (2002). Nuclear factor kappaB-dependent gene expression profiling of Hodgkin's disease tumor cells, pathogenetic significance, and link to constitutive signal transducer and activator of transcription 5a activity. J. Exp. Med. *196*, 605–617.

Holcik, M., Lefebvre, C.A., Hicks, K., and Korneluk, R.G. (2002). Cloning and characterization of the rat homologues of the Inhibitor of Apoptosis protein 1, 2, and 3 genes. BMC Genomics *3*, 5.

Infante, J.R., Dees, E.C., Olszanski, A.J., Dhuria, S. V, Sen, S., Cameron, S., and Cohen, R.B. (2014). Phase I dose-escalation study of LCL161, an oral inhibitor of apoptosis proteins inhibitor, in patients with advanced solid tumors. J. Clin. Oncol. *32*, 3103–3110.

Jakubowski, A., Ambrose, C., Parr, M., Lincecum, J.M., Wang, M.Z., Zheng, T.S., Browning, B., Michaelson, J.S., Baetscher, M., Baestcher, M., et al. (2005). TWEAK induces liver progenitor cell proliferation. J. Clin. Invest. *115*, 2330–2340.

Jones, N.C., Tyner, K.J., Nibarger, L., Stanley, H.M., Cornelison, D.D.W., Fedorov, Y. V, and Olwin, B.B. (2005). The p38alpha/beta MAPK functions as a molecular switch to activate the quiescent satellite cell. J. Cell Biol. *169*, 105–116.

Knapp, J.R., Davie, J.K., Myer, A., Meadows, E., Olson, E.N., and Klein, W.H. (2006). Loss of myogenin in postnatal life leads to normal skeletal muscle but reduced body size. Development *133*, 601–610.

Kottlors, M., and Kirschner, J. (2010). Elevated satellite cell number in Duchenne muscular dystrophy. Cell Tissue Res. *340*, 541–548.

Kristiansen, M., Graversen, J.H., Jacobsen, C., Sonne, O., Hoffman, H.J., Law, S.K., and Moestrup, S.K. (2001). Identification of the haemoglobin scavenger receptor. Nature *409*, 198–201.

Kuang, S. (2006). Distinct roles for Pax7 and Pax3 in adult regenerative myogenesis. J. Cell Biol. *172*, 103–113.

LaCasse, E.C., Mahoney, D.J., Cheung, H.H., Plenchette, S., Baird, S., and Korneluk, R.G. (2008). IAP-targeted therapies for cancer. Oncogene *27*, 6252–6275.

Liao, G., Zhang, M., Harhaj, E.W., and Sun, S.-C. (2004). Regulation of the NF-kappaB-inducing kinase by tumor necrosis factor receptor-associated factor 3-induced degradation. J. Biol. Chem. *279*, 26243–26250.

Loughna, P., Goldspink, G., and Goldspink, D.F. (1986). Effect of inactivity and passive stretch on protein turnover in phasic and postural rat muscles. J. Appl. Physiol. *61*, 173–179.

MAURO, A. (1961). Satellite cell of skeletal muscle fibers. J. Biophys. Biochem. Cytol. *9*, 493–495.

McLoon, L.K., and Wirtschafter, J. (2003). Activated satellite cells in extraocular muscles of normal adult monkeys and humans. Invest. Ophthalmol. Vis. Sci. *44*, 1927–1932.

Mendell, J.R., and Engel, W.K. (1971). The fine structure of type II muscle fiber atrophy. Neurology *21*, 358–365.

Miner, J.H., and Wold, B. (1990). Herculin, a fourth member of the MyoD family of myogenic regulatory genes. Proc. Natl. Acad. Sci. U. S. A. *87*, 1089–1093.

Mittal, A., Bhatnagar, S., Kumar, A., Paul, P.K., Kuang, S., and Kumar, A. (2010a). Genetic ablation of TWEAK augments regeneration and post-injury growth of skeletal muscle in mice. Am. J. Pathol. *177*, 1732–1742.

Mittal, A., Bhatnagar, S., Kumar, A., Lach-Trifilieff, E., Wauters, S., Li, H., Makonchuk, D.Y., Glass, D.J., and Kumar, A. (2010b). The TWEAK-Fn14 system is a critical regulator of denervation-induced skeletal muscle atrophy in mice. J. Cell Biol. *188*, 833–849.

Moss, F.P., and Leblond, C.P. (1971). Satellite cells as the source of nuclei in muscles of growing rats. Anat. Rec. *170*, 421–435.

Nagata, Y., Partridge, T.A., Matsuda, R., and Zammit, P.S. (2006). Entry of muscle satellite cells into the cell cycle requires sphingolipid signaling. J. Cell Biol. *174*, 245–253.

Novoyatleva, T., Diehl, F., van Amerongen, M.J., Patra, C., Ferrazzi, F., Bellazzi, R., and Engel, F.B. (2010). TWEAK is a positive regulator of cardiomyocyte proliferation. Cardiovasc. Res. *85*, 681–690.

Ogura, Y., Mishra, V., Hindi, S.M., Kuang, S., and Kumar, A. (2013). Proinflammatory cytokine tumor necrosis factor (TNF)-like weak inducer of apoptosis (TWEAK) Suppresses Satellite Cell Self-renewal through Inversely Modulating Notch and NF-κB Signaling Pathways. J. Biol. Chem. *288*, 35159–35169.

Oustanina, S., Hause, G., and Braun, T. (2004). Pax7 directs postnatal renewal and propagation of myogenic satellite cells but not their specification. EMBO J. *23*, 3430–3439.

Polek, T.C., Talpaz, M., Darnay, B.G., and Spivak-Kroizman, T. (2003). TWEAK mediates signal transduction and differentiation of RAW264.7 cells in the absence of Fn14/TweakR. Evidence for a second TWEAK receptor. J. Biol. Chem. *278*, 32317–32323.

Relaix, F. (2006). Pax3 and Pax7 have distinct and overlapping functions in adult muscle progenitor cells. J. Cell Biol. *172*, 91–102.

Rhodes, S.J., and Konieczny, S.F. (1989). Identification of MRF4: a new member of the muscle regulatory factor gene family. Genes Dev. *3*, 2050–2061.

Roos, C., Wicovsky, A., Müller, N., Salzmann, S., Rosenthal, T., Kalthoff, H., Trauzold, A., Seher, A., Henkler, F., Kneitz, C., et al. (2010). Soluble and transmembrane TNF-like weak inducer of apoptosis differentially activate the classical and noncanonical NF-kappa B pathway. J. Immunol. *185*, 1593–1605.

Rudnicki, M.A., Schnegelsberg, P.N., Stead, R.H., Braun, T., Arnold, H.H., and Jaenisch, R. (1993). MyoD or Myf-5 is required for the formation of skeletal muscle. Cell *75*, 1351–1359.

Schultz, E. (1996). Satellite cell proliferative compartments in growing skeletal muscles. Dev. Biol. *175*, 84–94.

Schuster-Gossler, K., Cordes, R., and Gossler, A. (2007). Premature myogenic differentiation and depletion of progenitor cells cause severe muscle hypotrophy in Delta1 mutants. Proc. Natl. Acad. Sci. U. S. A. *104*, 537–542.

Seale, P., Sabourin, L.A., Girgis-Gabardo, A., Mansouri, A., Gruss, P., and Rudnicki, M.A. (2000). Pax7 is required for the specification of myogenic satellite cells. Cell *102*, 777–786.

Shakhov, A.N., Collart, M.A., Vassalli, P., Nedospasov, S.A., and Jongeneel, C. V (1990). Kappa B-type enhancers are involved in lipopolysaccharide-mediated transcriptional activation of the tumor necrosis factor alpha gene in primary macrophages. J. Exp. Med. *171*, 35–47.

Sun, C., Cai, M., Gunasekera, A.H., Meadows, R.P., Wang, H., Chen, J., Zhang, H., Wu, W., Xu, N., Ng, S.C., et al. (1999). NMR structure and mutagenesis of the inhibitor-of-apoptosis protein XIAP. Nature *401*, 818–822.

Thomason, D.B., and Booth, F.W. (1989). Influence of performance on gene expression in skeletal muscle: effects of forced inactivity. Adv. Myochem. *2*, 79–82.

Tzankoff, S.P., and Norris, A.H. (1977). Effect of muscle mass decrease on age-related BMR changes. J. Appl. Physiol. *43*, 1001–1006.

Varfolomeev, E., Blankenship, J.W., Wayson, S.M., Fedorova, A. V, Kayagaki, N., Garg, P., Zobel, K., Dynek, J.N., Elliott, L.O., Wallweber, H.J.A., et al. (2007). IAP antagonists induce autoubiquitination of c-IAPs, NF-kappaB activation, and TNFalpha-dependent apoptosis. Cell *131*, 669–681.

Varfolomeev, E., Goncharov, T., Maecker, H., Zobel, K., Kömüves, L.G., Deshayes, K., and Vucic, D. (2012). Cellular inhibitors of apoptosis are global regulators of NF-κB and MAPK activation by members of the TNF family of receptors. Sci. Signal. *5*, ra22.

Vince, J.E., Wong, W.W.-L., Khan, N., Feltham, R., Chau, D., Ahmed, A.U., Benetatos, C.A., Chunduru, S.K., Condon, S.M., McKinlay, M., et al. (2007). IAP antagonists target cIAP1 to induce TNFalpha-dependent apoptosis. Cell *131*, 682–693.

Vince, J.E., Chau, D., Callus, B., Wong, W.W.-L., Hawkins, C.J., Schneider, P., McKinlay, M., Benetatos, C.A., Condon, S.M., Chunduru, S.K., et al. (2008). TWEAK-FN14 signaling induces lysosomal degradation of a cIAP1-TRAF2 complex to sensitize tumor cells to TNFalpha. J. Cell Biol. *182*, 171–184.

Wang, H., Hertlein, E., Bakkar, N., Sun, H., Acharyya, S., Wang, J., Carathers, M., Davuluri, R., and Guttridge, D.C. (2007). NF-kappaB regulation of YY1 inhibits skeletal myogenesis through transcriptional silencing of myofibrillar genes. Mol. Cell. Biol. *27*, 4374–4387.

Wiley, S.R., Cassiano, L., Lofton, T., Davis-Smith, T., Winkles, J.A., Lindner, V., Liu, H., Daniel, T.O., Smith, C.A., and Fanslow, W.C. (2001). A Novel TNF Receptor Family Member Binds TWEAK and Is Implicated in Angiogenesis. Immunity *15*, 837–846.

Wozniak, A.C., and Anderson, J.E. (2007). Nitric oxide-dependence of satellite stem cell activation and quiescence on normal skeletal muscle fibers. Dev. Dyn. *236*, 240–250.

Zammit, P.S., Relaix, F., Nagata, Y., Ruiz, A.P., Collins, C.A., Partridge, T.A., and Beauchamp, J.R. (2006). Pax7 and myogenic progression in skeletal muscle satellite cells. J. Cell Sci. *119*, 1824–1832.

Appendix
Table 2. Sequences of siRNAs used in 59-candidate siRNA screen

Target	Gene symbol	Dharmacon siRNA Catalog #	siRNA #	siRNA sequence
Non-targeting	N/A	D-001810-10	N/A	N/A
TNFSF-TNFRSF and alternative NF-κB				
TWEAK	TNFSF12	L-046846-01	1	UCGAAGAAGUGCUCCUAAA
			2	GAGCUAUUGCAGCCCAUUA
			3	CAGAGGAAAGCCAGGAUGU
			4	GGUACCUUUCUUGGAACAA
Fn14	TNFRSF12A	L-040436-01	1	AGACAGAGAGCCUCAAUCU
			2	CUAAGGAACUGCAGCAUUU
			3	GGAGGGAGACUUAUUAAUA
			4	GAUAUUUAUUGUGGGGAUA
TNF-α	TNFA	L-042302-00	1	GAAAGUCAACCUCCUCUCU
			2	GCCGAUGGGUUGUACCUUG
			3	GGGCAGGUCUACUUUGGAG
			4	CCAAAUGGCCUCCCUCUCA
TNFR1	TNFRSF1A	L-060201-01	1	GUAAAUACACUAAACGUCU
			2	GGAAGGAGUUCAUGCGUUU
			3	CAAUGCAGACCUUGCGAUU
			4	GGAGAAUAUCCUCGAGGCU
TRAF2	TRAF2	L-042814-01	1	GAGUCUACUUGAAUGGCGA
			2	CUGUCAUCGUGGCGGCAAA
			3	CGGAGUGUCCUGCAUGUAA
			4	AGUUCGGCCUUUCCAGAUA
TRAF3	TRAF3	L-040797-01	1	CUAGAGAACGGGACGUAUA
			2	CCUCACAAGUGCAGCGUUC
			3	GAAAUGUAACCCUUCGAUA
			4	GACAAGUACAAGUGCGAGA
TRAF6	TRAF6	L-042735-01	1	GCACAGCAGUGUAACGGGA
			2	GGACAAGGUUGCCGAAAUG
			3	GAGAACAGAUGCCUAAUCA
			4	GCUCAAUCGUUUAAUAAGA
TRAF7	TRAF7	L-054193-01	1	CCGGAAGGACCACGAGAGU
			2	GCCUAUACUUGGCGAGGGA
			3	CUUCAUACAUUGUCGGCAU
			4	CCUGAAAGAAUGCGAGCAC
TAK1	MAP3K7	L-040718-00	1	GGAUGGCGCCUGAAGUAUU
			2	CAGUAUGUCUUGUGAUGGA
			3	CUAACAUUGUCAAGUUGUA
			4	CCAGUGAGAUGAUCGAAGC
A20	TNFAIP13	L-058907-02	1	GCACCUAAGCCAACGAGUA

			2	GCUGUGAAGAUACGAGAGA
			3	AGAGACAUGCCUCGAACUA
			4	GCUCAACUGGUGUCGUGAA
PGC1a	PPARGC1A	L-040773-01	1	GAACAAGACUAUUGAGCGA
			2	UUACGCAGGUCGAACGAAA
			3	ACAAUGAGCCUGCGAACAU
			4	CAGCCGAGGACACGAGGAA
PGC1b	PPARGC1B	L-040905-01	1	UGGUACAGCUCAUUCGCUA
			2	GGGAAAAGCAAGUACGAAG
			3	GCUUUGAGGUGUUCGGUGA
			4	GGAAAAGGCCAUCGGUGAA
cIAP1	BIRC2	L-041990-00	1	GGAUAGAACACGCCAAAUG
			2	GAAUAGAAUGGCCCUCUUU
			3	GUCAGGAGUUUGUUGAUGA
			4	GCUCUAGCCCUCUUAAUUC
IKKα	CHUK	L-041014-00	1	GGAGAGACGUUAGCACAAA
			2	CCAUUGAUCUCUAUAAGCA
			3	AUAGUGAGCAGAUGACUUA
			4	GCAGCAAUGUUAAGUCUUC
RelB	RELB	L-040784-01	1	ACAUCGGAGCUGCGGAUUU
			2	GACCCGAUCUCCUGGACGA
			3	ACAUUAAGGAGAACGGCUU
			4	GGUGUGGACAAGAAGCGAA
p100	NFKB2	L-046030-01	1	GGAACAGCCCAAACAGCGA
			2	GCAGAUAGCCCACGUCAUU
			3	GUGCUCUGCUAGCGGGACA
			4	GGACAAUUGCUACGAUCCA
NIK	MAP3K14	L-040771-00	1	GAAAGAGCCCGUCCACCGA
			2	GCUAGAAGGUGGCUCGCUG
			3	GAACCGACCCUAGUCCUGU
			4	CUACUGACAUCCCGAGCUA
RIP1	RIPK1	L-040150-00	1	UCACCAAUGUUGCAGGAUA
			2	CCUCGUUGAUCGUGACUUU
			3	GAAGGCAUGUGCUACUUAC
			4	CAACCGCGCUGAGUACAAU
RIP2	RIPK2	L-052248-00	1	CAAAUUUCCCUCAGAAUAA
			2	ACGAGAAGCCGAAAUAUUA
			3	GCUCGACAGUGAAAGAAAU
			4	AUAUACAGCUAUGCAGUUA
RIP3	RIPK3	L-049919-00	1	UCAAGAUCGUGAACUCGAA
			2	CAAGUUCGGCCAAGUAUGA
			3	GGUAAAGCAUUAUCUGUCU
			4	ACACGGCACUCCUUGGUAU
IKKg/NEMO	IKBKG	L-040796-00	1	UAUGGACACUCUACAGAUA
			2	UGACAUCAUUGCUCGGAGA

			3	GGAAGAACCAGCUGAGUGA
			4	CUACAAGGCUGACUUCCAA
Other Cytokines				
IL4	IL4	L-043727-00	1	UCGAUAAGCUGCACCAUGA
			2	GAGAGAGAUCAUCGGCAUU
			3	CCAAGGUGCUUCGCAUAUU
			4	GCAAAUGGAUUACUCGUAG
IL4R	IL4R	L-043730-01	1	CUUAUUUACUUUCGGACUA
			2	UCACAUGCAUCCCGAGGAA
			3	UGGGAUAAGCAGACCCGAA
			4	AGGCUGAGCUUCCCGAUCA
IL13	IL13	L-046599-01	1	CAAACUAGAAACCGGAAAU
			2	GCAUUGAAGCAGUGGGCUC
			3	AUAGCUUAGCAAAGAGUUA
			4	AAGGUGAUGUGUAGUGAAU
IL13R	IL13RA1	L-041764-01	1	ACUCAAACCGACCGACAUA
			2	UCCAGAAACUCAUCGUAAA
			3	GAAAAUCUCUGCACGAUAA
			4	CAUCAGAACGUUCAAAUAA
MyD88	IL13RA2	L-046600-01	1	CGACUGAUUCCUAUUAAAU
			2	UGCCAGAAAUACUUAGGUA
			3	GCCUAUCGCUGUUCUUGAA
			4	GUUAGACCGUGAGGAUAUA
Calcineurin / NFAT				
NFATc1	NFATC1	L-054700-00	1	GAAUCGAGAUCACCUCCUA
			2	CCACAGGCCUCGUAUCAGU
			3	UAUACCAGCUCUGCCAUUG
			4	ACGGUUACUUGGAGAAUGA
NFATc2	NFATC2	L-054724-01	1	AGAUGAUCCUCACGGGCCA
			2	CUGACAUCGAGCUGCGGAA
			3	GCGCAGAGGCUUUGGUUGC
			4	GGAUUGAGGUCCAACCCAA
NFATc3	NFATC3	L-040068-02	1	CCUUAGAUGAUGUGAACGA
			2	GAAUGAAGCUGCUGCACGA
			3	AUAAUAUGUCAGCGAGUAU
			4	CAGAUAUAGAACUUCGAAA
NFATc4	NFACTC4	L-063420-01	1	GAGGACUUCUAGCGAGCAA
			2	AGACAUUGAGCUACGGAAG
			3	GCGGGAAGGUCGUGUCUGU
			4	CAGCUAGGUCGGUGAGGCU
NFAT5	NFAT5	L-058868-01	1	GGGCAAUGAUUCUGGUCGA
			2	AGAGUAACUGGGCGAAAUA
			3	CGGCAGGAGUGGAAGCGUU
			4	CCACUCAUAUCAAGCAGUA
Myoferlin	MYOF	L-057027-00	1	CUUCUAAGCUGUCGGAAAA

			2	UUAUAGAAGACACGAGAUA
			3	GUAAAUACCUGGCGAGAUC
			4	GGGAAUAUGCUUCGUUAAU
Beta-catenin factors				
GSK3b	GSK3B	L-041080-00	1	GGACCCAAAUGUCAAACUA
			2	CCACAGGAAGUCAGUUAUA
			3	UCAGAAGUCUAGCCUAUAU
			4	GAUUACACGUCCAGUAUAG
bCatenin	CTNNB1	L-040628-00	1	GUGAAAUUCUUGGCUAUUA
			2	GCGCUUGGCUGAACCAUCA
			3	CAGCAAAUCAUGCGCCUUU
			4	AAGCUGACCUGAUGGAGUU
Notch and target genes				
Notch1	NOTCH1	L-041110-00	1	CAAGAUUGAUGGCUACGAA
			2	GAGCGUAUGCACCACGAUA
			3	AGACAGCUAUGGUACUUAU
			4	GCCCGUGGAUUCAUCUGUA
Notch3	NOTCH3	L-047867-01	1	CCACGUGUCUUGACCGAAU
			2	GAACGUGUGUAGACGGUGU
			3	GCACUUUGUGUGAGCGAAA
			4	GGAAUAGGCUUUCGCUGCA
Jagged2	JAG2	L-043770-01	1	GCGAACUAGAGUACGACAA
			2	CCUCACGGGCACUGCGUUA
			3	GGGCACGUGCAUUGACGAA
			4	GGGCAUGUAGAGUGAUCGA
DLL1	DLL1	L-050912-01	1	GCCAAUUGCCAGCGCGAGA
			2	GUACAAAGGCACUUCGGGU
			3	GGUGUAAGAUGGAAGCGAU
			4	CCAAGUACCAGUCGGUGUA
Hes6	HES6	L-063093-01	1	CGAUGCUCCAACCGAAUUA
			2	GCUAGAGAACGCCGAGGUU
			3	AAUCCAUGCCGCUGCGUGA
			4	GGGCAGAAGUGGCCAAUCU
HeyL	HEYL	L-060622-01	1	GCUGUUGACUUCCGGAGUA
			2	CAAAUGGCAUCUACGCAAA
			3	CCCUGUUAUUCUAGUGAUA
			4	CGAUUGAAGUCCCCAGAUA
Pax7	PAX7	L-040966-01	1	CCUAGAAGAAGGCCGAUUU
			2	CCAAGAUUCUGUGCCGAUA
			3	UGACCAAUGUACACCGAUU
			4	GAGCAACAUUCCAACGCUU
Adhesion factors				
CD9	CD9	L-062029-01	1	CGGUCAAAGGAGGUAGCAA
			2	GACUCUAGACAUAAGAUAU
			3	CAUUUGUAGUUGAGGGAUC

			4	GCAAUGAAAGGUACUAUAU
CD81	CD81	L-062694-01	1	ACAAAGACCAGAUCGCCAA
			2	AGGCGUGAUCCUAGGUGUA
			3	AGCUGUACCUCAUUGGAAU
			4	GGACAUGGCCUGUGUAUAU
CD57	B3GAT1	L-050297-01	1	ACGUAGAGACACCACGCAA
			2	UAGUGUACUUCGCGGAUGA
			3	GGGACAUCCUUGCGAUUGU
			4	GGUCUGGCAUACACGAACA
CD36	CD36	L-062017-00	1	CCACAUAUCUACCAAAAUU
			2	GAAAGGAUAACAUAAGCAA
			3	AUACAGAGUUCGUUAUCUA
			4	GGAUUGGAGUGGUGAUGUU
Ia3	ITGA3	L-042246-01	1	GGACAAUGUUCGCGAUAAA
			2	GCUACAUGAUUCAGCGGAA
			3	AGACAUACCACAACGAGAU
			4	GCACACUGGUUCUAGGUCU
Miscellaneous				
Myomaker	TMEM8C	L-050810-01	1	GGGAUUACACCUACGUCCA
			2	GCCGUGACAUUCUGGAGUA
			3	GGUAUACUCCGGUCCCAUA
			4	GCGGCCUGUACAUGAGAAA
BAL1	PARP9	L-050249-01	1	CGUACACAUUUCAACGAUA
			2	CCAAAUAUGAUCUACGCAU
			3	CCAGACAGCUAUCGAAUUA
			4	ACACAAUGUCUUCGAAAUU
YY1	YY1	L-050273-00	1	ACAAUAGCUUGCCCUCAUA
			2	AGAACUCACCUCCUGAUUA
			3	GCUCAAAGCUAAAACGACA
			4	GUAAUAAGAAGUUUGCUCA
c-Myb	MYB	L-044112-00	1	CCGAAGCGUUGGUCUGUUA
			2	GAGACACUAUAACGACGAA
			3	GGAAAUACGUGAACGCGUU
			4	CAAAUAUUCUUACAAGCUC
FHL1	FHL1	L-045694-01	1	ACGAGAAGCAUAGGCGAUA
			2	CAUUAUAAGAAUCGCUACU
			3	UGUAAGAGUUGCAGCGGCU
			4	AGUAUUAAUCAACGAAGGA
Cell motility / migration				
Cdc42	CDC42	L-043087-01	1	AUAGAAACGCCUCGAUUAA
			2	GAAGGUGGGUGGACGCUGU
			3	GGCUGAAGCUUUCGCAAGA
			4	GGAUUAUGACAGACUACGA
RhoGDI	ARHGDIA	L-064240-00	1	CGACUGACCUUGGUAUGCA
			2	UCAAGUCGCGCUUCACAGA

			3	GAGAUCGUGUCCGGCAUGA
			4	GGUGUGGAGUACCGGAUAA
cRaf/Raf1	RAF1	L-040149-00	1	UCUUCUAGCUGAUGAUGUA
			2	GAUCAGCAAUGGCUUUGGA
			3	GGAUUUCGAUGUCAGACUU
			4	GCAGAGAGACUCGAGUUAU
Rac1	RAC1	L-041170-00	1	AGACGGAGCUGUUGGUAAA
			2	UGAGAACACCUAAGCACUA
			3	GCGUUGAGUCCAUAUUUAA
			4	GCAACUAGGUGUGCAAAUC
FAK	PTK2	L-041099-00	1	GAAGUUGGGUUGUUUGGAA
			2	GGGCAUCAUUCAGAAGAUA
			3	GCUCCAGAGUCAAUCAAUU
			4	GUACAGCACUCGCGUAUCU
Src	SRC	L-040877-00	1	GCACGGGACAGACCGGUUA
			2	GGGAGCGGCUGCAGAUUGU
			3	UCAGAUCGCUUCAGGCAUG
			4	GCUCGUGGCUUACUACUCC
FRNK	PTK2B	L-040719-00	1	GACACUACCUGGAACGAAA
			2	UCAUGGAACUGUAUCCUUA
			3	UAAGGGCUCUCUCAUCAUG
			4	GAAGUUGGCUCAGCAGAAC

Table 3. Primer sequences for TWEAK, Fn14, and B2M used in RT-qPCR analyses

Target	Primer	Sequence (5'-3')	Amplicon size (bp)
TWEAK (TNFSF12A)	Forward	GGACAGGATGGAGCACAAG	125
	Reverse	CCAGCCCTGATGACTGTAAAT	
Fn14 (TNFRSF12A)	Forward	CTAGTTTCCTGGTCTGGAGAAGATG	76
	Reverse	CCCTCTCCACCAGTCTCCTCTA	
B2M	Forward	GGCCTGTATGCTATCCAGAA	198
	Reverse	GAAAGACCAGTCCTTGCTGA	